Circulation Copy

Communications Research Centre

A RADIO NOISE ANALYZER

by

W.R. LAUBER AND J.M. BERTRAND

LIBRARY
C.R.L. 2733
C.R.C.
DEPT. OF COMMUNICATIONS

IC

CRC TECHNICAL NOTE NO. 696

Department of Communications
Ministère des Communications

LKC
TK
5102.5
.R48e
#696
c.2
c.b

OTTAWA, JANUARY 1979

COMMUNICATIONS RESEARCH CENTRE

DEPARTMENT OF COMMUNICATIONS
CANADA

Industry Canada
Library - Queen

MAR 2 0 2013

Industrie Canada
Bibliothèque - Queen

A RADIO NOISE ANALYZER

by

W.R. LAUBER AND J.M. BERTRAND

(Radio and Radar Branch)

COMMUNICATIONS CANADA
C. R. C.
LIBRARY - BIBLIOTHÈQUE

CRC TECHNICAL NOTE NO. 696

January 1979
OTTAWA

CAUTION
This information is furnished with the express understanding that:
Proprietary and patent rights will be protected.

DD 2113084
DL 5368130

TK 5102.5
R48e
#696
c.b

TABLE OF CONTENTS

COMMUNICATIONS CANADA
C. R. C.
LIBRARY - BIBLIOTHÈQUE

A RADIO NOISE ANALYZER

by

W.R. Lauber and J.M. Bertrand

ABSTRACT

This report describes equipment which has been constructed at the Communications Research Centre (CRC) to measure statistical distributions of radio noise. The Analyzer in its present configuration may be used with either of two receivers, thus giving a frequency coverage from 150 kHz to 1 GHz. The equipment can make measurements of Amplitude Probability Distribution's (APD's) and Average Crossing Rate (ACR) characteristics; however, plans are given for modifying the equipment to enable measurements of Pulse Spacing and Pulse Duration Distributions. The results of system-performance tests for both gaussian and impulse noise are given. Appendices are included which describe the detailed circuitry and the operational procedures of the Analyzer.

1. INTRODUCTION

Radio noise measurements have consumed large amounts of effort during past years, but a unified, internationally-accepted approach to obtain information useful for environmental prediction and system performance has yet to be achieved in the EMC community. Two types of information are required; 1) a knowledge of the characteristics of the radio environment, and 2) a knowledge of the behaviour of the communication system operating in this radio environment. Since radio noise, whether man-made or natural is a random process, it can only be described in probabilistic or statistical terms and cannot be represented by a deterministic waveform or any collection of deterministic waveforms. Since about 1945, Statistical Communication Theory has developed as a method of describing random-non-deterministic

processes in mathematical terms. In the 1950's, the British [1,2]; the Americans [3,4]; and the Japanese [5], developed equipment to make statistical measurements of atmospheric noise. In the 1960's, developing technology brought about equipments using low-power integrated-circuits to replace most vacuum tube systems. The Institute for Telecommunication Sciences (ITS) was thus able to develop an equipment denoted as a DM-2 (Distribution Meter). This device was used in a Radio Noise Mobile Laboratory [6,7] to measure Amplitude Probability Distributions (APD's) and Average Crossing Rate (ACR) characteristics of atmospheric and man-made noise. A later version of this device called a DM-3 was built for the US Air Force as part of noise characteristic measurement system. The equipment described in this report is based very heavily on the DM-3 design [8].

Section two presents a brief description of statistical noise theory as it pertains to the radio noise Analyzer. A general description of the equipment and a block diagram are presented in Section three. The results of system performance tests to both gaussian and impulsive noise are presented in Section four. Finally, Section five presents some proposed extensions of the equipment. Two Appendicies give the detailed circuitry of the equipment and a description of the operating procedures for the equipment, when it is used in a system configuration.

2. STATISTICAL NOISE THEORY

Man-made radio noise, whether originating from a single vehicle ignition system or from a collection of many different sources, is a random process. This means that it can only be described in probabilistic or statistical terms. Thus, we shall discuss briefly the probabilistic descriptions that are useful in communication-system design and analysis.

A random process, X(t) is completely described by its hierarchy of density distributions:

$P_1(x_1, t_1)dx_1$ is the probability of finding X(t) between x_1 and $(x_1 + dx_1)$ at time t_1 (1)

$P_2(x_1, t_1; x_2, t_2)\, dx_1 dx_2$ is the joint probability of finding X(t) in the range $(x_1, x_1 + dx_1)$ at time t_1 and in the range $(x_2, x_2 + dx_2)$ at time t_2, (2)

and so on.

These statistics are referred to as ensemble statistics since they assume an ensemble of waveforms. However, in real life we have only one waveform; i.e., the one our measurement instrument received. Thus, the required statistics are ensemble statistics and the measured ones are time averages of a single member of the ensemble. For practical purposes, to correct this problem, we assume the process is stationary which means that

$P_1(x_1,t_1)$ is not a function of time t, and that $P_2(x_1,t_1;x_2,t_2)$ is only a function of the time difference $t_2 - t_1$.

Since man-made noise is basically non-stationary, great care must be taken in making measurements. We must make our measurements over a long enough time period to obtain a good estimate of the required parameter but be relatively certain that the noise process remains stationary during this time period. Kanda [9] in 1974 showed that Allan variance analysis [10] could be used to estimate the time of stationarity of a man-made noise process. Thus, we usually assume that the random process is stationary enough to obtain the required statistics. We are, however, interested in how these statistics change with time, date and location.

Although a random process, X(t), is completely described by its hierarchy of distributions, there are other statistical properties that are important to communication systems which are not immediately implied by this hierarchy. Distributions of level crossings of X(t) within a time interval and distributions of the time intervals between successive crossings are examples of this.

For a communications system, the random noise process of interest is the one seen by that part of the receiving system which is extracting the information from the received waveform, (i.e., after the IF in a receiver). We are usually interested in a narrowband process, where the pass-band of the system is a small fraction of the received frequency. The noise process X(t) at the output of a narrowband filter is given by:

$$X(t) = V(t)\cos(w_c t + \phi(t)) \tag{3}$$

where w_c is the received frequency in radians/sec,
$V(t)$ is the envelope process,
$\phi(t)$ is the phase process.

An example of this is given in Figure 1. For man-made noise processes in the absence of discrete signals, $\phi(t)$ is uniformly distributed with a probability density function $p(\phi)$ given by:

$$P(\phi) = \frac{1}{2\pi}, \quad -\pi \leq \phi < \pi$$

The required statistics that determine the performance of a communication system are, in general, envelope statistics* thus we will consider only the envelope process V(t).

One of the most useful envelope statistics is the amplitude characteristic usually referred to as the Amplitude Probability Distribution, $P_0(V)$, (APD). This is related to the first order density distribution p(v) by:

$$P_0(V) = 1 - P(V) = \int_V^\infty p(v)dv \tag{4}$$

where V is the voltage level, and
P(V) is the Probability Distribution which represents the probability that V(t) is less than or equal to V.

* *The only exceptions to this statement are phase-modulated systems; e.g., Phase-shift-keying systems.*

The APD, $P_0(V)$, represents the probability that V(t) exceeds some level V. For example, if X(t) is a "White" Gaussian noise process, i.e.

$$p(x) = \frac{1}{\sqrt{\pi N_0}} \exp-\left[\frac{x^2}{N_0}\right] \tag{5}$$

where N_0 is the normalized single sided noise power spectral density (watts/Hz)

then the envelope V(t) is Rayleigh [11], with probability density function:

$$p(v) = \frac{2v}{N_0} \exp - \left[\frac{v^2}{N_0}\right] \tag{6}$$

and the APD is

$$P_0(V) = \exp - \left[\frac{V^2}{V^2_{rms}}\right] \quad V \geq 0 \tag{7}$$

Figure 2 shows an example of the envelope of a man-made radio-noise process and shows definitions of the various statistical distributions to be discussed. As was mentioned above, the value of the APD $P_0(V_i)$ is the fraction of the total measurement time, T, for which the envelope exceeded level V_i. It can also be seen that the value of the APD for the lower level V_{i-i} is larger than for level V_i.

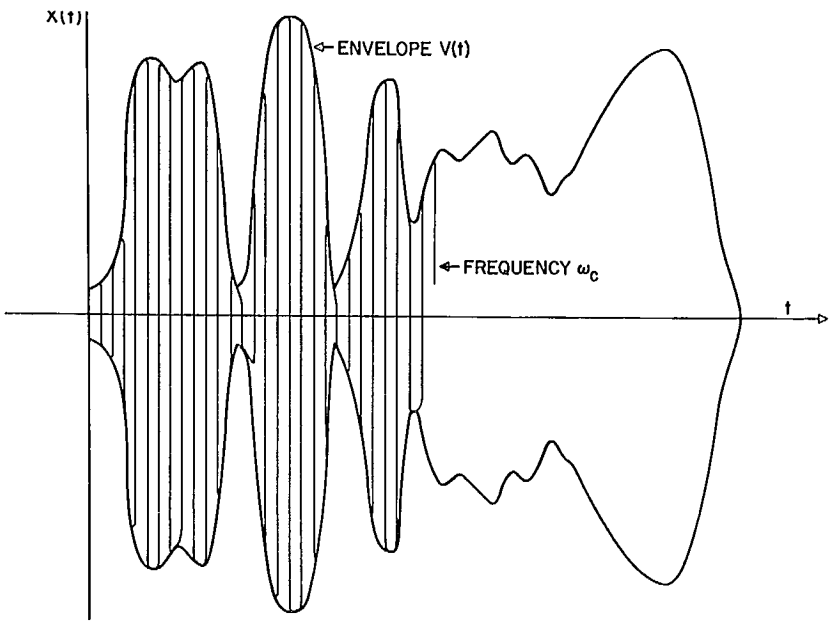

Figure 1. An Example of Noise Process at Output of Narrowband Filter

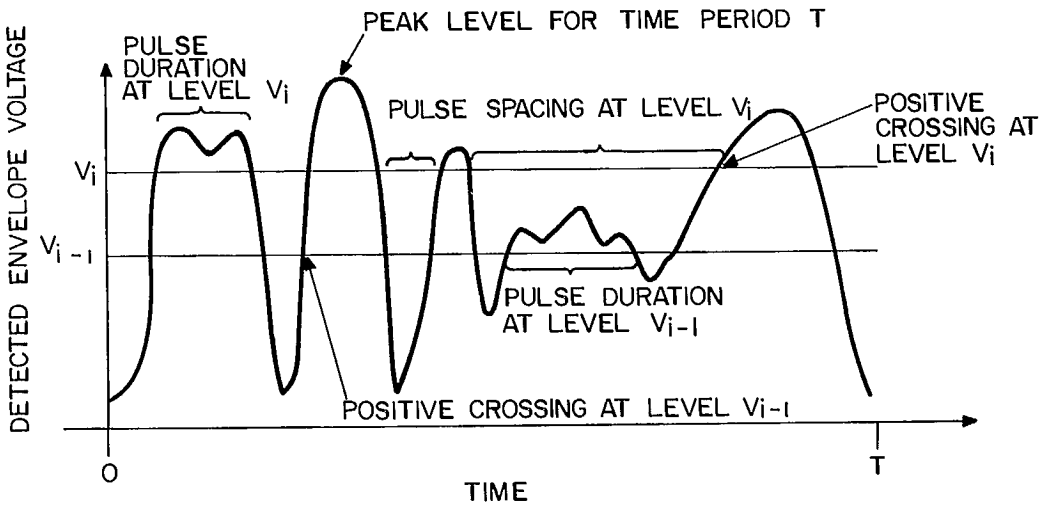

Figure 2. An Example of Envelope of Man-Made Radio Noise Process

The average crossing rate, ACR, characteristic is the average number of positive crossings of given levels by the noise envelope per unit time. When there is a dominant periodic pulse in the noise process, the ACR will be equal to its pulse repetition rate and the envelope of the noise exceeding level V is composed of isolated impulse responses (i.e., non-overlapping pulses). The maximum number of positive crossings depends upon the receiver bandpass and noise characteristics. The average crossing rate characteristic presents the average number of times the noise envelope crosses various levels and is given as positive crossings per second versus envelope voltage level.

The Pulse Spacing Distribution (PSD) for level V_i is the fraction of pulse spacings at level V_i that exceeds time τ. Thus, the PSD is a function of the random variable τ. Likewise, the Pulse Duration Distribution (PDD) for level V_i is the fraction of pulse durations at level V_i that exceeds time τ.

Given the APD data, any noise parameter that is a function of the envelope amplitude may be calculated; V_{rms}, $V_{average}$, V_d and possibly V_{peak}. Expressions for the first three are given below [12].

$$V_{average} = - \sum_{i=1}^{N-1} V_i \Delta P_0(v_i) \text{ volts} \tag{8}$$

$$(V_{rms})^2 = - \sum_{i=1}^{N-1} V_i^2 \Delta P_0(v_i) \text{ volts}^2 \tag{9}$$

where $V_i = v_i + \frac{\Delta v}{2}$

v_i is the i^{th} measured level threshold voltage (volts)

and $v_{i+1} > v_i$

$\Delta v = (v_2 - v_1)$ (assuming the v_i are all equidistant)

$\Delta P_0(v_i) = (P_0(v_{i+1}) - P(v_i))$

$P_0(v_i)$ is the measured probability that the i^{th} threshold value is exceeded

N is the total number of threshold levels for which we have $P_0(v_i)$ data

$$V_d = 10 \log (V_{rms})^2 - 20 \log (V_{average}) \text{ dB} \quad (10)$$

To estimate a value of V_{peak}, we must set some probability threshold; i.e., V_{peak} is the level that is exceeded 0.0001% of the time. For a V_{peak} measurement one must also state the duration of the observation time during which the peak value was observed, since "theoretically" there is no such thing as the "peak" value of a random noise process; i.e., there is always some finite probability that any level will be exceeded.

The ACR data is not only of a physical and theoretical interest but also of considerable practical importance. A paper by Blake and Lindsey [13] discusses the level crossing problem in great detail as well as giving an extensive bibliography of the work in this area. Our prime interest is to measure the ACR characteristic and try, if possible, to relate it back to the physical process as a pulse repetition rate. It is also very useful in testing of mathematical models of man-made radio noise processes.

3. GENERAL DESCRIPTION OF EQUIPMENT

3.1 BLOCK DIAGRAM

The Radio Noise Analyzer (RNA) uses an envelope detector to detect the IF output voltage and quantize it into 15 discrete levels spaced 6 dB apart. In the APD mode, the percentage of time that the IF envelope exceeds each quantizer level is computed. In the ACR mode, the number of times per second that the IF envelope crosses each quantizer level in the positive direction is computed.

The block diagram in Figure 3 shows that the equipment may be divided into six main sections; detector, digitizer, accumulator, sampling, timing and control, and finally display and output. In the following parts we give a general description of each section, however, Appendix A gives a complete description of the circuitry used in the RNA.

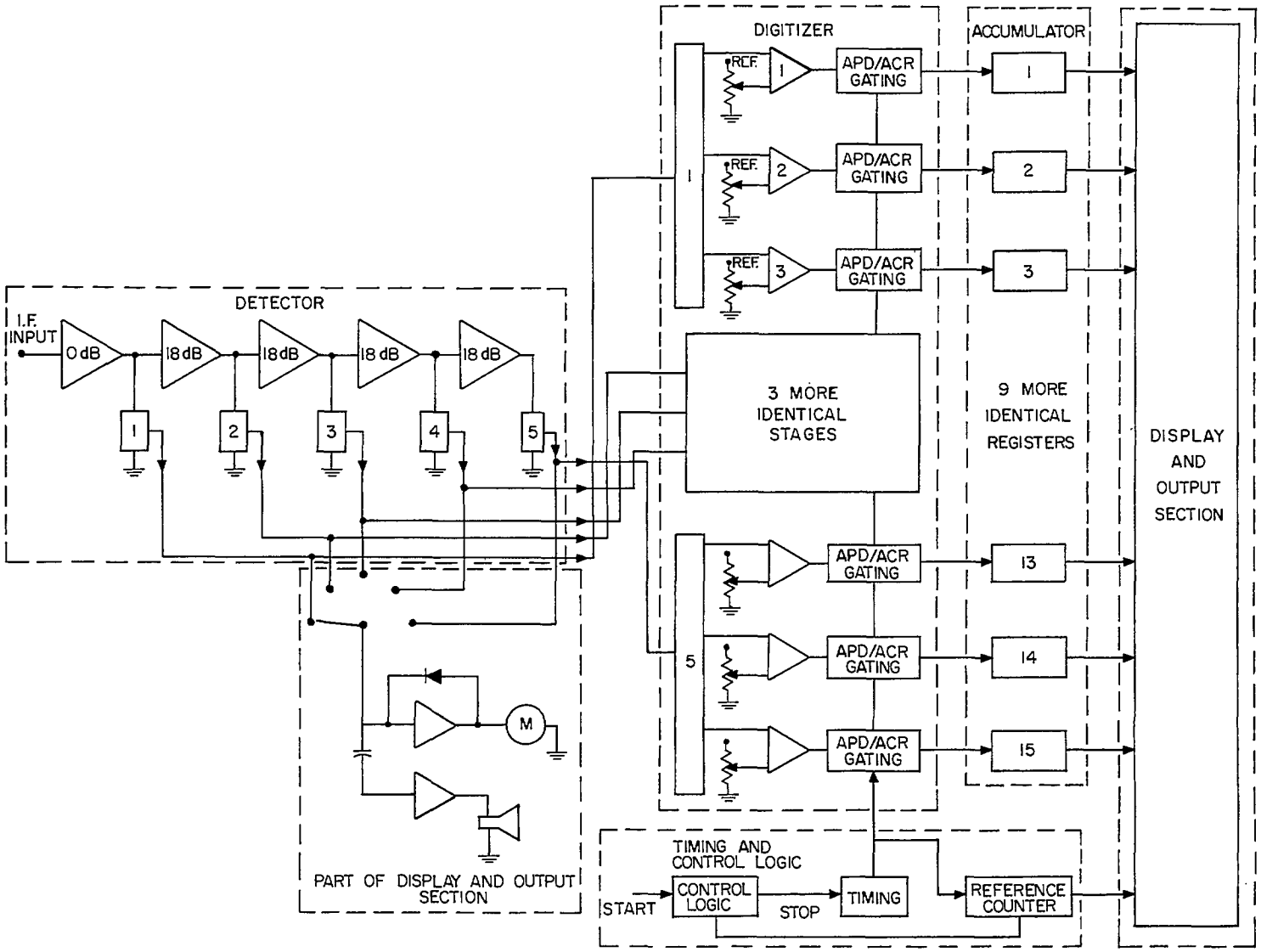

Figure 3. Block Diagram of the Radio Noise Analyzer

3.2 THE DETECTOR SECTION

The detector section is contained on a single card. There are presently two available for the equipment, one for an IF frequency of 455 KHz and a 6 dB bandwidth of 25 KHz and the other for an IF frequency of 20.5 MHz and a 6 dB bandwidth of 2 MHz. Since it is difficult to build a single stage detector with a 90 dB dynamic range, the detector consists of five stages each with a dynamic range of 18 dB. This large dynamic range is necessary because it has been shown by Matheson [14] that the APD of man-made radio noise may have a large dynamic range (e.g., 86 dB between the level that was exceeded 99 percent of the time and the level that was exceeded 0.0001 percent of the time). The IF circuitry of the receiver will usually limit the dynamic range to less than 90 dB. The five outputs are each split into three levels each 6 dB apart. This arrangement adds gain to the low amplitude portion of the dynamic range which makes it easier to build the quantizer circuits.

3.3 THE DIGITIZER SECTION

The digitizer section consists of two cards; a quantizer card and a gating card. The quantizer card is made up of 15 fast acting comparators. One of the two inputs for each comparator is connected to a detector output and the other to an adjustable voltage source. When the detected output exceeds the reference voltage the comparator output becomes a binary "1" otherwise it is a "0".

The mode of the analyzer (either APD or ACR) is selected by a switch on the front panel of the gating card. In the APD mode the output of each quantizer is sampled at a rate selected on the sampling card. As long as the detected IF level exceeds a quantizer reference level, counts are added to the respective register at the sampling rate. To reduce the possibility of the quantizer switching state during a sample pulse, a very short aperture time (approximately 130 nsec) is used. In the ACR mode whenever the detected IF voltage exceeds a particular quantizer level, the output of that quantizer goes from "0" to a "1". The transition causes only one count to be added to the respective level counter no matter how long the detected level remains below or above the quantizer reference. The length of time for the distribution in the ACR mode is selected on the sampling card by a combination of the RATE and AUTO SHUT OFF switches (e.g., a distribution would be measured in 100 seconds at a "RATE" of 10 KHz and "AUTO SHUT OFF" of 10^6).

3.4 THE ACCUMULATOR SECTION

The accumulator section consists of 15 identical cards. Each card (register) is made up of 10 cascaded decade counters (wired to give a maximum count of 4×10^9). The input to each register is a series of binary "1's" from its corresponding digitizer section. The output, 38 bits in BCD format, are fed to a bus system for the display and/or the output device.

3.5 THE TIMING AND CONTROL SECTION

The timing and control section consists of three cards; a sampling card, a reference counter card, and a control card. The sampling card performs three functions; start command, sample timing pulses for the gating card, and automatic shut-off for the sampling pulses. The start command is derived from the COUNT-MANUAL STOP-RESET switch on the front panel of the sampling card. The sampling pulses are derived from a 2 MHz oscillator and a divider chain, which gives a sampling rate of 2 MHz, 1 MHz, 500 kHz, 200 kHz, 100 kHz, 50 kHz, 5 kHz or 2 kHz. The desired sampling rate is selected by a switch on the front panel of the sampling card. The number of samples, or the length of time when used in conjunction with the sampling rate for each distribution, may be selected from 10^5, 10^6, 10^7, 10^8, or 10^9 samples. Thus when the desired number of samples have been collected, as computed from the reference counter, the automatic shut off function stops the data collection process. The switch also positions the decimal point on the display for the APD mode only.

The reference counter card is similar to the cards in the accumulator section except that the 9 to 0 transitions from counters 5,6,7,8, and 9, are used for the automatic shut off function. It receives its input from the gating card but its gating card circuitry does not have an input from the quantizer card.

The control card acts as a controller for the output device (presently a 16 digit FLUKE printer) and the display. It contains the circuitry to select each of the 15 registers of the accumulator and the reference counter in sequence and to output the register identification and contents to the printer.

3.6 THE DISPLAY AND OUTPUT SECTION

The display and output section consists of a number of cards that: 1) control the display of the register data; 2) act as an interface to the output device; and 3) monitor the input signal. The output of each register is fed on a common data bus through two stages of level converters to the ten digit numeric display. Each register is selected either by a set of switches located on the front panel or by the control card, and its contents are placed on the common data bus for display and output to the printer.

A detector monitoring card is also a part of this section. The detector output that gives the best reproduction and audio level of the input signal is selected from the five-position switch on the front panel of this card. There is an audio output for earphones and a meter whose output is linear in dB to monitor the input level. This card is not in the data path and is only a convenience to the operator for monitoring the input signal.

4. SYSTEM PERFORMANCE TESTS

The Radio Noise Analyzer was designed to be operated with either of two standard field intensity meters; namely Singer NM-26T and NM 37/57*. The first receiver covers the frequency range 150 kHz to 32 MHz and has an IF

* *The RNA is presently compatible with any receiver with a 455 kHz or a 20.5 MHz IF frequency output.*

frequency of 455 kHz and a bandwidth of 4 kHz. The second receiver covers the frequency range 30 MHz to 1 GHz and has an IF frequency of 20.5 MHz with bandwidths of 10 kHz, 100 kHz and 1 MHz. It is possible to operate the RNA with either receiver by simply plugging in the corresponding detector card and recalibrating the gating card. Presently, we have two 90 dB dynamic range detector cards, one for an IF frequency of 455 kHz and the other for an IF frequency of 20.5 MHz. These two cards were designed so that measurements made with the RNA would primarily be limited by the receiver IF filter bandwidth and dynamic range characteristics. This section will describe the results of tests using the two receivers for both gaussian and impulse noise.

4.1 CALIBRATION

The radio noise analyzer is calibrated with a CW signal from a signal generator which is tuned to the detector frequency. By adjusting the potentiometers on the gating card we can set the levels at which the 15 comparators switch, 6 dB apart. When the receiver is connected to the RNA, a signal generator is used again and tuned to any convenient RF frequency to determine what RF input level is required to exceed each of the 15 levels in the RNA. The NM-26T receiver must be operated in a fixed gain mode (i.e. Peak) with no AGC (AGC action would tend to compress the measured APD). The gain of the receiver is controlled by the receiver attenuator and "Peak Pot" so that the APD is centred within the dynamic range of the RNA i.e., not saturating at the top end or in the set-noise at the bottom. The IF output of the NM-37/57 receiver is before the AGC loop thus this receiver may be operated in any mode and is independent of the RNA. The gain of this receiver is controlled by the receiver attenuator and the CAL adjustment.

4.2 TESTS

There are two basic types of Middleton's Class B [15, 16] noise (noise that is spectrally very broad with respect to the receiving system) that have been dealt with in the literature; namely gaussian and impulsive noise. Most radio environments are usually some combination of the above noise types and are between the two extremes of galactic noise (which is gaussian) and vehicle ignition noise (which is impulsive). We have tested the equipment's response to both gaussian and impulsive noise.

Figure 4 shows a number of APD's of gaussian noise measured at 2.5 MHz from a Gaussian Noise Generator using the Singer NM-26T receiver and the 455 kHz detector card. The abscissa of the graphs gives the percentage of time that each receiver level (dB) was exceeded. The graph paper used here is Rayleigh paper, thus the APD of the noise envelope of gaussian noise, which is Rayleigh-distributed, will plot as a straight line with slope of $-\frac{1}{2}$. This type of graph paper has been used extensively in the literature [7, 9, 17]. Each of the six measured APD's shown in the figure consist of 10^6 samples using the 20 kHz sampling rate. The theoretical APD's are straight lines with a slope of $-\frac{1}{2}$ and they intersect the V_{rms} measured on the receiver at a probability level of 36.8% (from Equation 7, P_0 ($V_{rms} = e^{-1}$)).

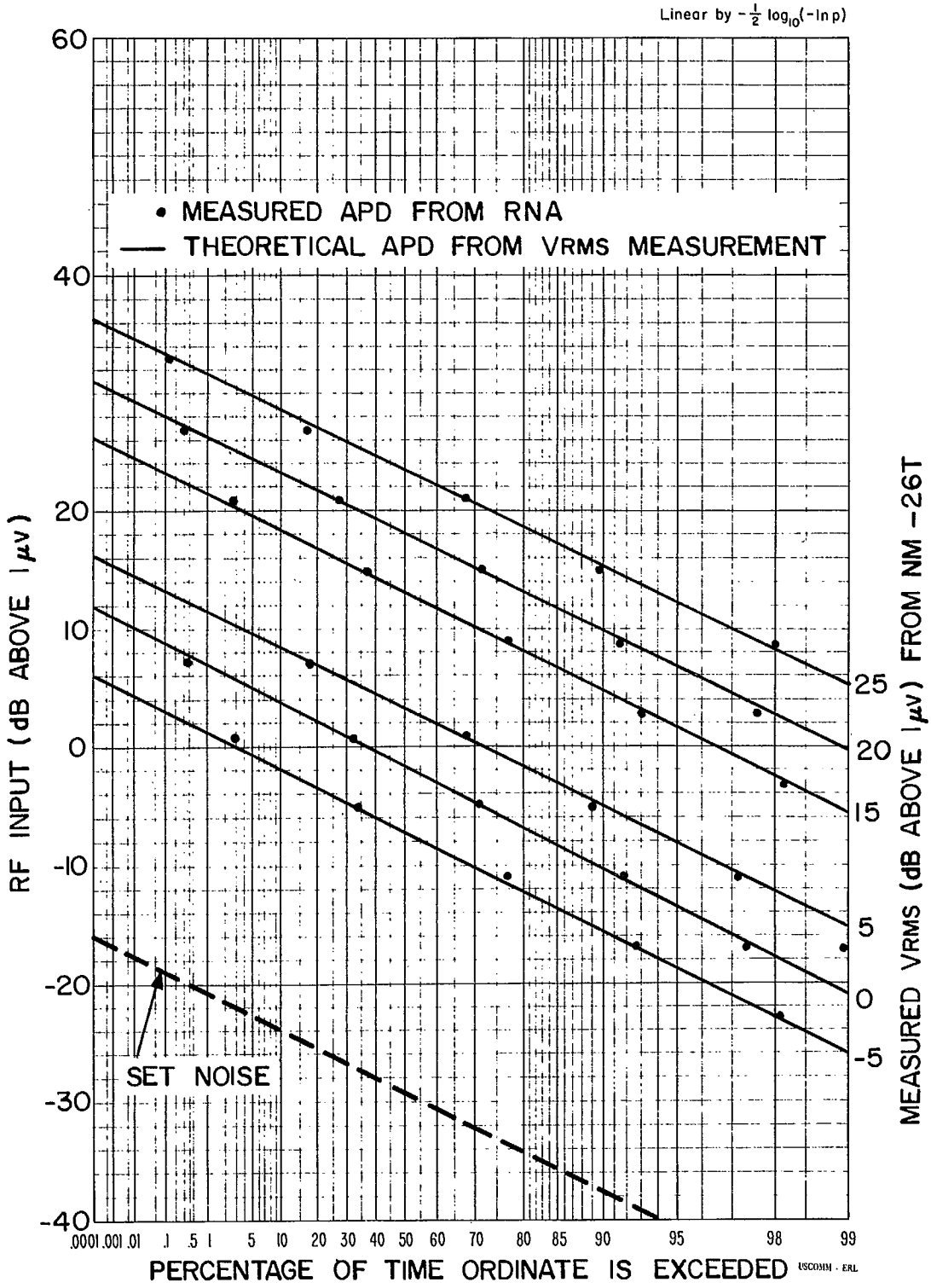

Figure 4. Amplitude Probability Distributions of Gaussian Noise at 2.5 MHz

Also on the figure is a line marked "SET NOISE". This is the system noise threshold and was measured by terminating the receiver input with a 50 ohm resistor. The receiver noise is also gaussian in character.

Also by using Equations 9 and 10 we were able to compute values for V_{rms} and V_d for each APD. Table 1 shows the results of comparing the computed V_{rms} with that measured on the NM-26T, and the computed V_d with the theoretical value of 1.05 for gaussian noise. (The V_d meter on the NM-26T read 1 dB for these tests.) The calculated values all compare favourably with the measurements and theory.

Figure 5 shows three APD's of gaussian noise taken with the Singer NM 37/57 receiver and the 20.5 MHz detector card at 140 MHz. The APD's were measured with the three different bandwidths of the receiver. The theoretical APD's were derived from the computed values of V_{rms}.* Also included in the figure are the three APD's representing the system noise threshold for the three bandwidths.

---

* *When the measurements were taken, there was no equipment available to measure V_{rms} and V_d directly. Subsequently, an rms converter has become available* [*18, 19*].

TABLE 1a

Comparison Between V_{rms} Measured on NM-26T and V_{rms} Calculated from APD Data

Measured V_{rms} on NM-26T (dB above 1 μv)	Frequency (MHz) 1.5	2.5	5.0
-5.0	-5.7	-5.6	-5.5
0.0	0.2	0.2	0.2
5.0	4.7	4.8	4.7
15.0	14.5	14.6	14.4
20.0	20.2	20.2	20.1
25.0	24.8	24.8	24.7

TABLE 1b

Comparison Between Theoretical Value of V_d for Gaussian Noise and Value of V_d Calculated from APD Data

Theoretical Value of V_d for Gaussian Noise	Frequency (MHz) 1.5	2.5	5.0
1.05	1.17	1.18	1.18
1.05	1.21	1.21	1.21
1.05	1.13	1.13	1.13
1.05	1.16	1.15	1.17
1.05	1.20	1.18	1.21
1.05	1.13	1.12	1.13

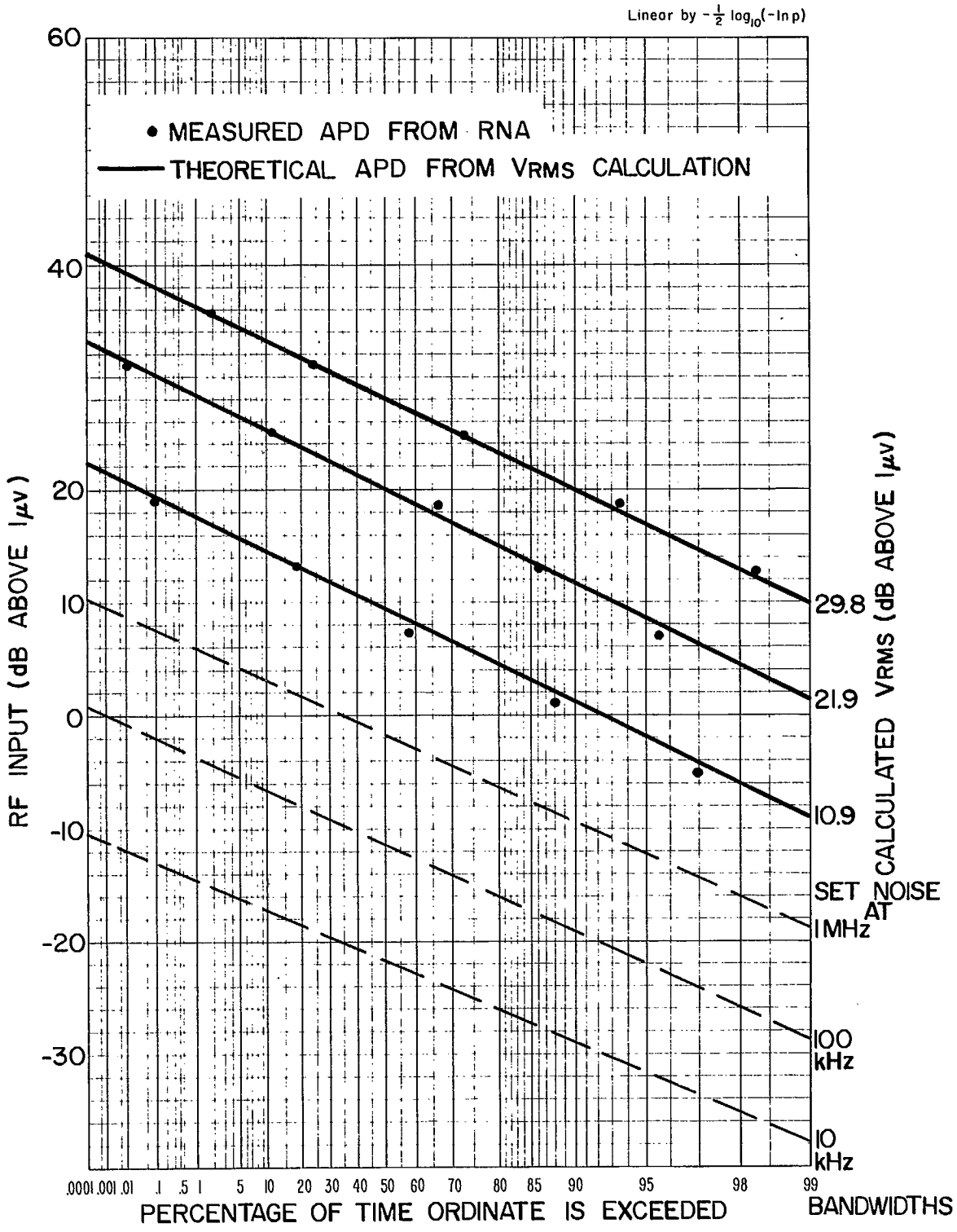

Figure 5. Amplitude Probability Distributions of Gaussian Noise at 140 MHz

One of the objectives of our radio noise program is to show the possibility of relating statistical measurements to the physical characteristics of the man-made noise process. This can be shown dramatically with impulsive noise. A particular APD may be measured from an infinite number of different time waveforms. However, if one also measures the time characteristics of a noise process, it becomes possible to characterize the noise process in a way which is much more useful for mathematical modelling purposes.

An impulse generator produces a periodic train of very narrow pulses at a fixed amplitude. If these are fed into the input of a receiver, the IF amplifier, because of its limited bandwidth response, produces a "stretched" pulse at the detector.

Figure 6 shows the impulse response of a particular Singer NM-26T receiver which has an impulse bandwidth of 5.2 kHz, and the impulse responses of the three bandwidths of a particular Singer NM 37/57 receiver. These show that the IF response of the NM-26T receiver is nearly Gaussian (i.e. only one zero crossing) whereas the IF response of the NM 37/57 receiver is not Gaussian (i.e. three zero crossings). This may be important since the shape of the IF filter response is known to have a large effect on the measured APD's. These responses show the extent to which each IF bandwidth "stretches" the received impulse. At low repetition rates, when the time between pulses is greater than the pulse length, the receiver response is a series of nonoverlapping pulses. However, at high repetition rates, i.e. when the time between pulses is less than or equal to the pulse width, the receiver has not fully responded to a first pulse when a second pulse comes along, thus the receiver response is the sum of the two responses; i.e. overlapping pulses. We are presently only interested in the low repetition rate case. The envelope of the noise in the time period between pulses, i.e. "y - x" in Figure 6 will have a Rayleigh amplitude distribution and the time period denoted by x in the figure is, by definition, the impulsive component of the entire noise process. Thus, we can calculate the ratio (x/y) of impulsive noise to Gaussian noise of this input noise process. Figure 7 shows a typical family of APD's for impulse repetition rates of 100 - 1000 IPS. These were measured with the NM-26T receiver. Similar results have been obtained from the three bandwidths of the NM 35/57 receiver. As we have discussed, the low levels follow a Rayleigh distribution; the higher levels, although linear, are at a much steeper slope thus not from gaussian noise. Of importance here is the break point (BP) between the gaussian and impulsive components of the APD. As we predict, the break points shift to the higher probabilities with increasing repetition rate. Table 2 shows the comparison between the predicted ratio of impulsive to gaussian for each repetition rate with the measured probability from the APD at the break point for the four presently available IF bandwidths.

NOTE: A large number of different time waveforms could produce the same effect, only the ratio is important.

Also for the measured APD's it is possible by means of Equations 9 and 10, to compute values for the V_{rms} and V_d noise parameters and for the NM-26T receiver we were able to compare these calculated values with those measured on the receiver. Table 3 shows the results of this comparison.

By comparing Tables 1 and 3 we can see that the impulse response comparison is not as good as the gaussian but is well within the ± 2 dB error of the receiver. As was stated previously, a true radio environment is

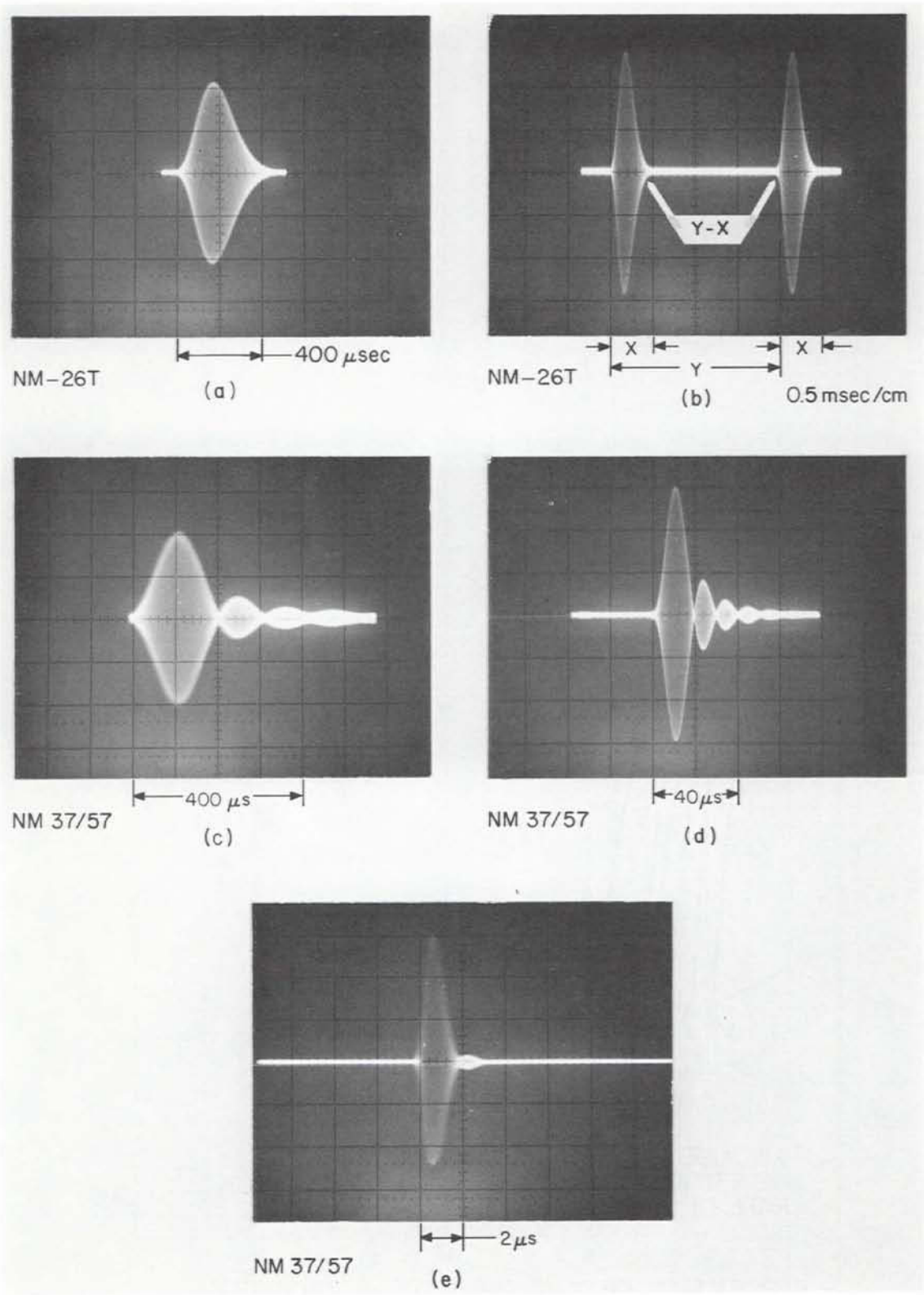

Figure 6. IF Impulse Responses of Singer NM-26T and NM 37/57 Receivers

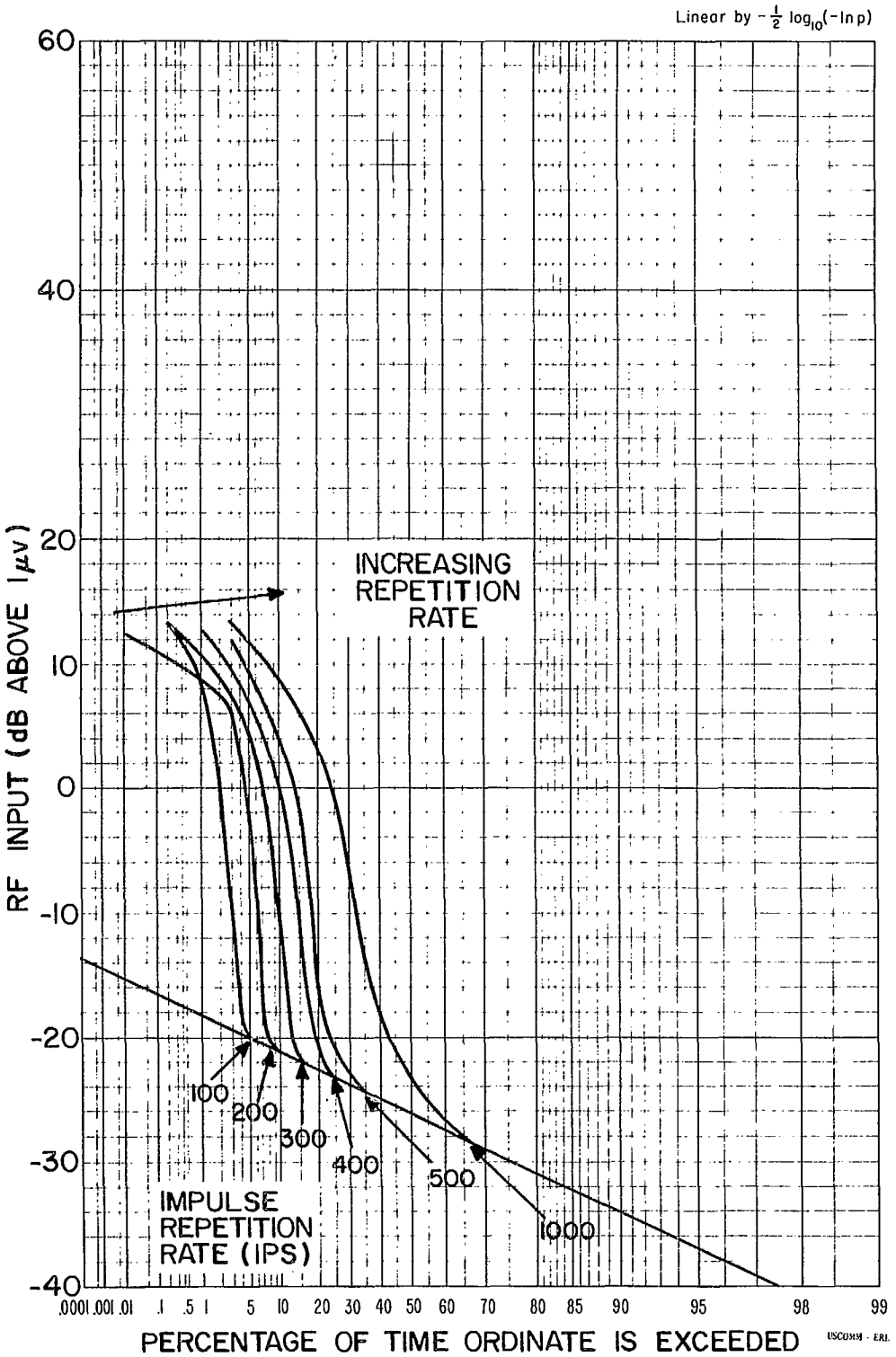

Figure 7. Typical Family of Amplitude Probability Distributions for Impulse Noise

TABLE 2

Comparison Between the Theoretical Ratio of Impulse to Gaussian Noise % Theory and the Probability Measured at the Break Point % (Measured)

Impulse Repetition Rate (IPS)	NM-26T 5.2 kHz BW		10 kHz BW		NM 37/57 100 kHz BW		1 MHz BW	
	Theory	Measured	Theory	Measured	Theory	Measured	Theory	Measured
100	3.9	4.1	4	3.5	0.4	0.42	0.02	0.02
200	7.7	8.4	8	7.0	0.8	0.86	0.04	0.04
300	11.6	11.6	12	10.6	1.2	1.3	0.06	0.06
400	15.4	15.4	16	14.0	1.6	1.7	0.08	0.08
500	19.3	19.7	20	17.8	2.0	2.1	0.10	0.10
600	23.1	23.5	24	21.4	2.4	2.6	0.12	0.12
700	26.9	27.6	28	25.0	2.8	3.1	0.14	0.13
800	30.8	31.3	32	28.4	3.2	3.6	0.16	0.15
900	34.7	34.9	36	32.4	3.6	3.8	0.18	0.17
1,000	38.5	38.8	40	36.1	4.0	4.2	0.2	0.20
2,000					8.0	8.4	0.4	0.38
3,000					12.0	12.7	0.6	0.60
4,000					16.0	17.0	0.8	0.79
5,000					20.0	21.1	1.0	1.00
6,000							1.2	1.20
7,000							1.4	1.39
8,000							1.6	1.59
9,000							1.8	1.78
10,000							2.0	2.00

TABLE 3

Comparison Between Measured V_{rms} and V_d Data and that Calculated from APD Curves

Impulse Repetition Rate (Hz)	V_{rms}		dB Difference	V_d		dB Difference
	NM-26T	RNA		NM-26T	RNA	
100	-6.8	-8.6	1.8	10.7	11.1	0.4
200	-3.0	-4.1	1.1	9.3	10.2	0.9
300	-2.2	-2.9	0.7	8.1	9.4	1.3
400	-2.2	-2.3	2.1	7.4	8.8	1.4
500	0.8	-0.6	1.4	6.7	7.8	1.1
600	1.8	-0.1	1.9	6.1	7.3	1.2
700	2.4	0.7	1.7	5.6	6.8	1.2
800	3.0	1.4	1.6	5.0	6.2	1.2
900	3.5	1.7	1.8	4.7	6.0	1.3
1,000	4.0	2.3	1.7	4.3	5.4	1.1

usually partially gaussian and partially impulsive and these tests give the system response to the two extremes. Figure 8 shows the values of V_{rms} calculated from the APD data versus the impulse repetition rates for the four bandwidths. True values of V_{rms} are only found in the linear portion of the curves. A theoretical line with slope of 10 dB per decade is also shown through the data. Deviation of the data from the theoretical slope at low repetition rates is caused by set noise limiting in the IF portion of the receiver. This shows that when making measurements one should have some idea

of the received waveform because of the limitation of the measuring equipment.

Finally, it was stated that the ACR characteristic is one measure of the time characteristics of the input noise process. Figure 9 shows the family of corresponding ACR's for the APD's impulsive component of the noise. Table 4 shows the results of comparing the input repetition rate with that measured by the ACR at one level (6 dB) above the break point on the APD characteristic. The measured impulse rates are generally higher than the input values especially for the lower bandwidths. These "false" counts are caused by low probability high amplitude pulses occurring in the gaussian noise part of the noise waveform.

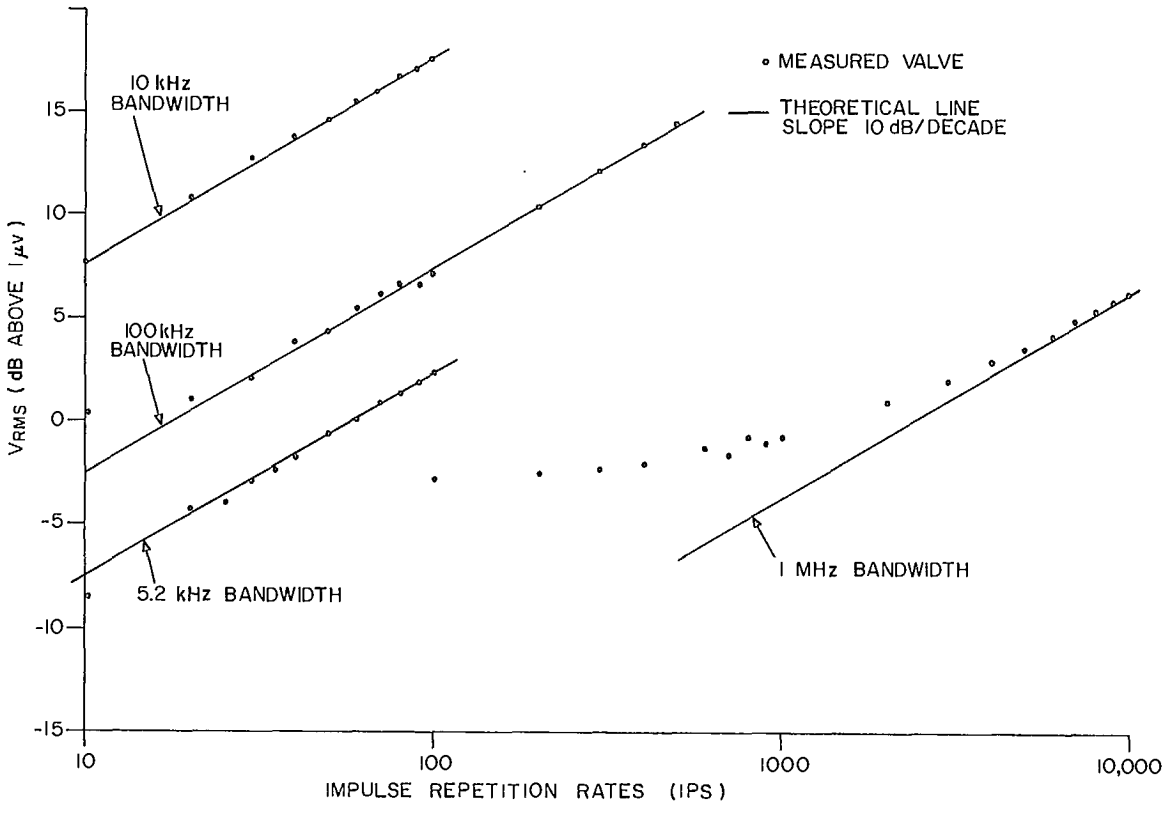

Figure 8. Calculated V_{rms} Values Versus Impulse Repetition Rates

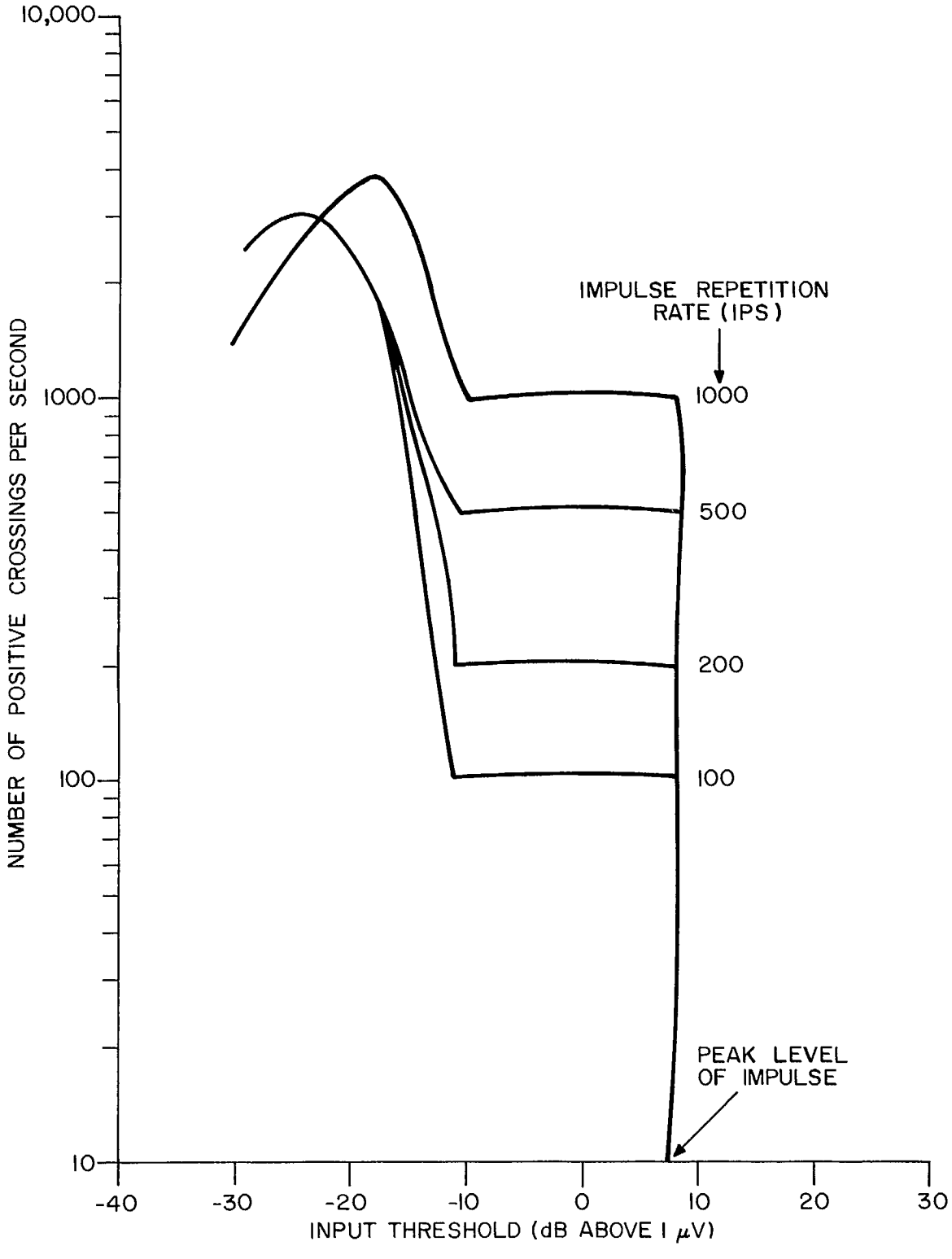

Figure 9. Typical Family of Average Crossing Rate Characteristics for Impulse Noise

TABLE 4

Measured Impulse Repetition Rates of Noise

Impulse Repetition Rate (IPS)	NM-26T		NM 37/57	
	5.2 kHz BW	10 kHz BW	100 kHz BW	1 MHz BW
100	102	101	100	100
200	200	200	200	199
300	310	302	300	300
400	412	402	400	399
500	516	503	501	499
600	619	604	599	599
700	724	705	699	699
800	825	803	798	799
900	932	906	902	899
1,000	1031	1005	1000	1000
2,000			2000	1999
3,000			2999	3001
4,000			4002	4001
5,000			5001	5000
6,000				5999
7,000				7000
8,000				8000
9,000				8998
10,000				9997

5. PROPOSED EXTENSIONS

The modular construction of the equipment makes it relatively easy to change its configuration by replacing certain cards. We have shown in Section 3 that, by merely replacing detector cards (and recalibrating the quantizer card) the equipment will operate with different receivers.

We are also interested in measuring Pulse Spacing (PSD) and Pulse Duration (PDD) Distributions with this equipment. To date, these have been computed only on a large computer from a digitized analog tape of a radio noise sample.

At present, by combining the results of the APD and ACR data at each level we can compute average pulse spacings and average pulse duration.

$$\text{AVPD } (V_i) = \frac{\text{total time level } V_i \text{ is exceeded}}{\text{Number of positive crossing of level } V_i}$$

$$= \frac{\text{probability that level } V_i \text{ is exceeded}}{\text{number of positive crossings of level } V_i \text{ per unit time}}$$

The average pulse spacing is the inverse of this, i.e.

$$\text{AVPS } (V_i) = \frac{1 - \text{probability that level } V_i \text{ is exceeded}}{\text{number of positive crossings of level } V_i \text{ per unit time}}$$

If man-made noise were composed of pulses occurring randomly according to a Poisson distribution we could use the above expression, especially at the higher envelope levels, with an exponential model to predict the Pulse Duration and Pulse Spacing Distributions. Some recent data by Spaulding and Disney [7] tend to show that there may be some correlation in the noise process which could severely restrict the use of the above simplified model. To date there is a very limited amount of data available with which such a decision may be made.

We may obtain the PSD and PDD data by simply replacing the gating card. Figure 10 shows a proposed circuit that would enable us to measure four pulse spacings or durations at three levels simultaneously (each level uses five registers). The 16th or reference register would be used to determine the length of time for each distribution. As one can see from the Figure, four of the five registers count the number of pulse spacings or durations that exceed specified lengths and the fifth register counts the total number of pulses crossing the level. To obtain points for the distribution, one must divide the count in each of the four registers by that in the fifth, to give the percentage of pulse spacings or durations which exceed specified times.

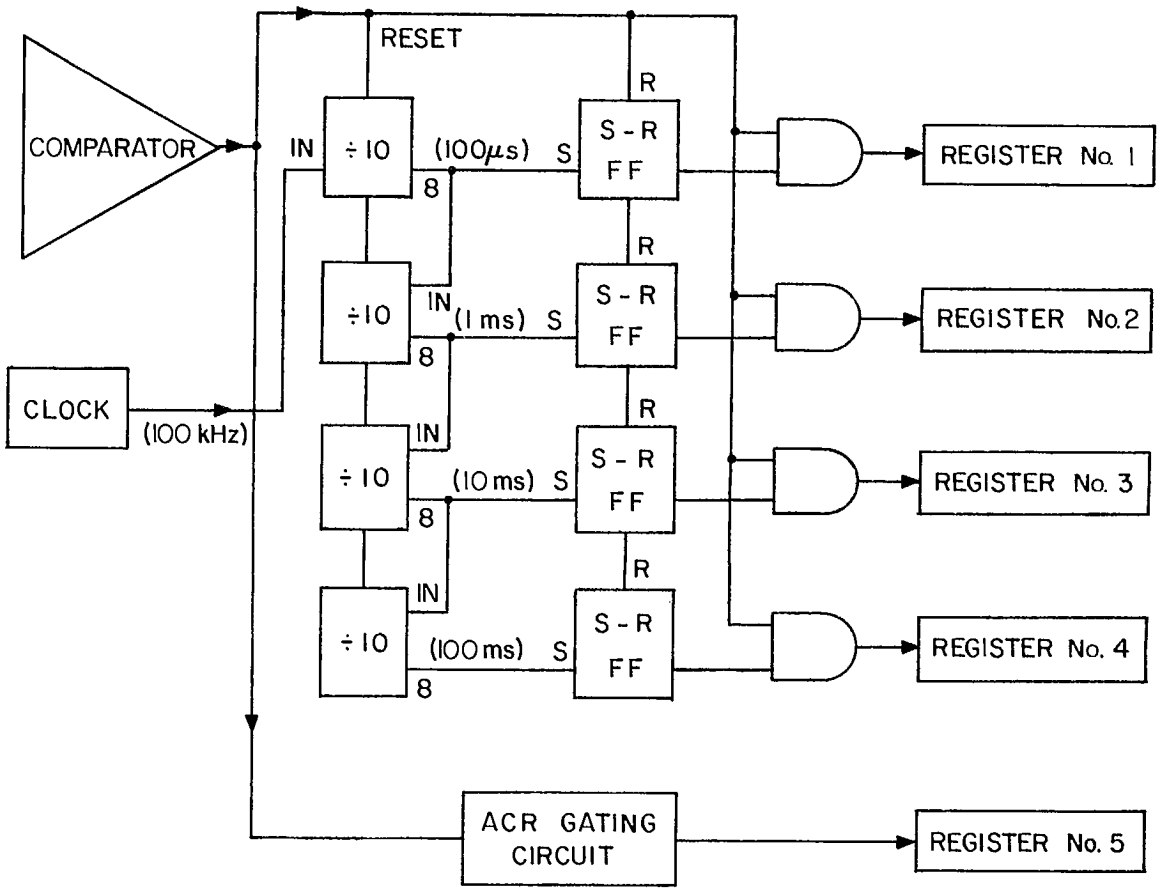

Figure 10. Proposed Pulse Duration Distribution Circuit

For pulse durations, the circuit operates as follows: When the level is exceeded the comparator output goes to a logical "1". This resets the flip-flops (FF) and enables the divide by 10 circuits to receive clock inputs at say the 100 kHz rate. After 100 μsec the first flip-flop is set, after 1 msec the second is set and so on. When the input signal falls below the threshold of the comparator its output goes to a logical "0". This stops the clock pulses and gates the outputs of the flip-flop into the respective registers. One count is also added to register 5 by the ACR circuit. For example if the pulse had a duration of 12 msec a single count would be gated into the first three registers and a zero into the fourth. Also if the duration were only 0.8 msec a single count would be gated into only the first register and zeros into the other three. For measuring pulse spacings (the inverse of pulse durations) an inverter would be placed after the comparator so that the counting circuit would be energized when the input level fell below the threshold and de-energized when the threshold was again exceeded. To accommodate various possible pulse widths there would also be a switch provided to vary the input clock rate; i.e., with a 100 kHz clock input we are able to measure pulse widths of 100 μsecs and 1, 10 and 100 msec, however with a 1 MHz clock input we could measure pulse widths of 10 and 100 μsec and 1 and 10 msec.

Since all statistical data must be read into a computer before it can be used, a major addition to this equipment would be a digital output device, e.g., magnetic tape, a 32 bit word computer (single precision) or a 16 bit word computer (double precision) would easily contain the maximum register count of 4×10^9.

6. REFERENCES

1. Harwood, J., C. Nicolson, *Atmospheric Radio Noise (Equipment for the Measurement of Amplitude Distributions)*, Electronic Radio Engineer, Vol. 35, pp. 183-190, May 1958.

2. Clarke, C., *Atmospheric Noise Structure Measuring Equipment for 15 kHz-20 MHz*, Electronic Thechnology, Vol. 37, pp. 197-204, May 1960.

3. Hoff, R.S., R.C. Johnson, *A Statistical Approach to the Measurement of Atmospheric Noise*, Proceedings of the IRE, Vol. 40, pp. 185-187, February 1952.

4. Watt, A.D., E.L. Maxwell, *Measured Statistical Characteristics of VLF Atmospheric Radio Noise*, Proceedings of the IRE, Vol. 45, pp. 55-62, January 1957.

5. Yuhora, H., T. Ishida, M. Highashimura, *Measurement of Amplitude Probability Distributions of Atmospheric Noise*, Journal of Radio Research Laboratories Japan, Vol. 3, p. 101, 1956.

6. Disney, R.T., R.J. Matheson, A.D. Spaulding, *Radio Noise Measuring and Analysis Facility*, Institute for Telecommunication Sciences, Boulder, Colorado, November 1971.

7. Spaulding, A.D., R.T. Disney, *Man-made Radio Noise Part 1: Estimates for Business, Residential and Rural Areas*, OT Report 74-38, June 1974.

8. Matheson, R.J., *Operational Manual for DM-3*, July 1972, to be published by the National Telecommunications and Information Administration, Boulder, Colorado.

9. Kanda, M., *Time and Amplitude Statistics for Electromagnetic Noise in Mines*, National Bureau of Standards Report NBSIR 74-378, June 1974.

10. Allan, D.W., *Statistics of Atomic Frequency Standards*, Proceedings of the IEEE, Vol. 54, No. 2, pp. 221-230, February 1966.

11. Middleton, D., *Introduction to Statistical Communication Theory*, McGraw-Hill Book Company, New York 1960.

12. Spaulding, A.D., Private Communication.

13. Blake, I.F., W.C. Lindsey, *Level Crossing Problems for Random Processes*, IEEE Transactions on Information Theory, Vol. IT-19, No. 3, pp. 295-315, May 1973.

14. Matheson, R.J., *Instrumentation Problems Encountered Making Man-Made Electromagnetic Noise Measurements for Predicting Communication System Performance*, IEEE Transactions on EMC, Vol. EMC-12, No. 4, pp. 151-158, November 1970.

15. Middleton, D., *Statistical-Physical Models of Man-Made Radio Noise Part 1, First-Order Probability Models of the Instantaneous Amplitude*, Office of Telecommunications Report 74-36, April 1974.

16. Spaulding, A.D., D. Middleton, *Optimum Reception in an Impulsive Interference Environment*, Office of Telecommunications Report 75-67, June 1975.

17. Shepherd, R.A., *Measurements of Amplitude Probability Distributions and Power of Automobile Ignition Noise at HF*, IEEE Transactions on Vehicular Technology, Vol. VT-23, No. 3, August 1974.

18. McLeish, C.W., R. Misner, *Instrument for RMS and Average Envelope Measurement of Narrow Band IF Waveform*, National Research Council Report No. ERB-895, Ottawa, April 1976.

19. Brancker, R.W.S., W.R. Lauber, *Direct V_{rms} and V_d Measurement of the Urban VHF/UHF Radio Environment*, Paper No. 77032 presented at the International Electrical, Electronics Conference and Exposition, Toronto, September, 1977.

20. Spaulding, A.D., *Man-Made Noise, the Problem and Recommended Steps Toward Solution*, Office of Telecommunications Report 76-85, Boulder, Colorado, April 1976.

21. Bolton, E.C., *Comparative Statistics of Atmospheric Radio Noise and Man-Made Noise Below the HF Band*, Paper presented at the Second Symposium and Technical Exhibition on Electromagnetic Compatibility, Montreux, Switzerland, June 1977.

(THIS PAGE INTENTIONALLY LEFT BLANK)

APPENDIX A

Detailed Circuitry of the Radio Noise Analyzer

A.1 INTRODUCTION

As discussed in Section 3, the RNA basically consists of 5 main sections: 1) the detector, 2) the digitizer, 3) the accumulator, 4) the sampling, timing and control circuitry, and 5) the display and output control circuitry. This Appendix will describe the circuits used in each section.

The design architecture of the RNA is identical to the DM-3 which was designed and built at the ITS Laboratory in Boulder, Colorado [8, 20]. Although the design and operation of the RNA is the same, there are some changes that make this unit different; e.g., it has two different detector boards which enable operation with more than one specific receiver, a calibrator is not built into our unit, also the circuitry on the Meter/Audio board is different. It must be emphasized that the theoretical concepts behind the RNA and the DM-3 are identical and that the output quantities are compatible, i.e., in the APD mode, the percentage of time that specific envelope amplitude levels are exceeded are calculated and in the ACR mode the number of positive crossings of the envelope voltage at each threshold in a specified time is calculated. The IF filter characteristics that effect the APD and ACR measurements are completely determined by the receiver to which the RNA is coupled [21]. Figure A1 is a photograph of the front panel of the RNA showing the different plug-in cards, and Figure A2 is a photograph of the inside of the RNA showing the physical layout of the printed-circuit cards.

A.2 DETECTOR

Since some examples of radio noise have had a dynamic range of the order of 80-90 db [14], the detector was required to have 90 db of linear dynamic range. However, because of the limited dynamic range of the analog comparators in the digitizer section (which follows) we were required to build a five-stage detector with each stage having 18 dB dynamic range. This requirement not only simplified the design of the detector but also gave additional gain to the low amplitude portion of the dynamic range, bringing it equal in amplitude to the high portion of the dynamic range. The RNA has two different detector cards, one for an IF frequency of 455 KHz and one for an IF frequency of 20.5 MHz. The basic design of the two is the same. Figure A3 is a basic schematic of the detector circuit. The five amplifiers are RCA CA3028A RF amplifier integrated circuits. This circuit provides two isolated outputs, one is used to drive the next stage and the other drives the detector for the present stage. Except for the first one, they are all set for a gain of 18 dB between stages. The first stage transforms the 50 ohm input impedance to the high impedance used in the circuit with very low

gain. The final stage is terminated in a fixed load resistor. The detector output of each stage is a DC voltage of 0-0.5V. For a low input signal, the last stage output is used but for a large input signal the output from the first stages are used with outputs from the final stages being saturated at 0.5V.

Figures A4 and A5 are detailed schematics of the two detector cards. A transformer is used in the between-stage tuned circuits. The bandwidth of this circuit was kept sufficiently narrow to minimize the probability of noise saturating the final stage, but broad enough to pass the input bandwidth.

The major architectural differences between the two detector cards are in the output detector parts (IF to DC transformation).

The emitter-base junction of the 2N2189 transistor acts as the detector diode for the 455 KHz detector. The high impedance of the tuned circuit gives the detector increased dynamic range by allowing even small IF levels to exceed the threshold voltage of the diode. As well, the transistor is biased like a common base amplifier with the common base current gain equal to one. The current detected by the emitter-base diode goes to the collector thus the transistor looks like a high impedance current source. A three section RC low-pass filter is used to eliminate the 455 KHz ripple frequency.

A hot carrier diode (HP2800) is used as the rectifying element for the 20.5 MHz detector. A tuned toroidal transformer feeds the diode, providing good signal to noise ratio and keeping the diode in its linear operating range. The RC filter smooths the rectified signal.

Each detector section is loaded with a resistor chain consisting of three resistors which provides a signal for the comparators on the quantizer card. These resistors are physically located on the quantizer card. The values were computed to give the same voltage, 125 mV., at each comparator. Different values of resistors are used for the two detectors. For the 455 KHz detector the values are, 100, 51 and 51 ohms and for the 20.5 MHz detector the values are, 4.7K, 2.4K and 2.4K ohms.

The main objective, when calibrating the detector card, is to get the detector threshold levels to be 6 dB apart. Since the set noise level was around 20 dB above 1 μv the maximum detected level must be 20 + 90 = 110 dB above 1 μv for the 90 dB of the linear dynamic range. Initially, C1 was adjusted for maximum signal transfer (impedance matched to 50 ohms input). Next the interstage tuning capacitor was adjusted for maximum signal transfer within the bandwidth limitations. Finally, the combination of R1 (the RF gain control) and R2 (the RF attenuator) was adjusted to give the desired interstage gains. A large signal, say 110 dB above 1 μv, was fed into the detector and the output of the first stage was checked to be 0.5V. The input was decreased by 18 dB and the output of the second stage was set at 0.5V by adjusting R1 and R2. This was repeated for stages three, four and five. If the set noise level is reached before stage five, one must start with a higher input level for stage one. The attenuator (R2) is only used for fine adjustments as it introduces noise into the system and should be set as low as possible. Since there is some interaction between the various controls, it is advisable to repeat the adjustments several times.

Figures A6 and A7 show the measured I/O characteristics of the two detector cards with a separate curve for each stage. Also marked on the curves are the thresholds for the 15 analog comparators which are set at 6 dB intervals.

A.3 DIGITIZER

This section consists of two cards (the quantizer and the gating card). Some detector circuitry (i.e., the resistor loading chains) is also located on the quantizer card. Figure A8 is a block diagram of the digitizer circuitry. As shown in the Figure, there are 15 similar circuits, one for each of the detector levels. We shall only describe the operation of one level since all 15 are the same.

The output of the analog comparator (SN5271ON) is a logical "1" whenever the detected output is above the threshold set by the 1K 10-turn potentiometer located on the front panel of the quantizer card, otherwise, the comparator output is a logical "0". The gating card has two modes: Amplitude Probability Distribution (APD) and Average Crossing Rate (ACR). The mode is selected by a toggle switch located on the front panel, which switches a "COUNT-ENABLE" signal (0 - count, 1 - Reset), which enables one of the two sides of the gating chip (½ N8440A) when a distribution is being taken. In the ACR mode, a count is produced at the output every time the detector level is exceeded, i.e., when the comparator output goes from a 0 to a 1. In this mode, the comparator output is routed directly to the registers.

In the APD mode, the comparator output is sampled through a D-type flip-flop at a fixed rate determined by the sampling pulses. Figure A9 is a timing diagram of this sampling operation. The sampling pulses are in the form of a square waveform which are inverted to form the CLOCK waveform. The CLOCK $+\Delta T$ signal is a short (130 nSEC) pulse from a oneshot that triggers on the trailing (falling) edge of a sampling pulse. This is the "CLK" signal for the flip-flop. When the CLR input is "high" then the "CLK" pulse clocks the D input to the Q output of the flip-flop. The D input comes from the comparator. The minimum switching time of the input signal is 1/BW (1 μSEC). The aperture is approximately one-tenth of this minimum switching time thus the input cannot change state while being sampled.

The last line of the timing diagram shows the Q output for both input states. A count is added to the register when the Q output goes from "0" to a "1". The output stays high until the clear (CLOCK) input goes low and then falls to "0". During the second pulse, the Q output remains low since the input is low. Thus, every time the comparator threshold is exceeded when a sampling pulse occurs, a count is added to the register.

The remaining ½ N8440A chip (7½ are used for the 15 levels) is used to gate the sampling pulse to the reference counter. In the APD mode, it is used to count the total number of samples in the distribution. In the ACR mode, it still counts sampling pulses which may be used to time the distribution. For example, if the sampling rate is 100 KHz, the length of the sample is 1, 10, 100 or 1,000 seconds depending on the setting of the AUTO SHUT-OFF at 10^5, 10^6, 10^7, or 10^8 counts respectively. The output data may be scaled by the appropriate factor of 10 to give the crossing rate in crossings/second.

A.4 ACCUMULATOR

The accumulator consists of 16 identical cards, one for each detector level and one for the reference register. Each register consists of 10 decade counters (SN74L90N) and provides a 38 bit BCD output capable of counting up to 3,999,999,999. The low power chips were used to conserve power since these chips draw one-tenth the current of the normal chip. The overall current drain of the accumulator is 600 ma rather than 6 amps at 5 volts. Figure A10 is a schematic of a register card. Before each distribution is taken, the reset line from the sampling card is energized to clear the accumulator (all the counters of all the registers). This sets all the outputs to a "1". The first count into a register starts at 0 thus each register is always one count low. This error is insignificant for 10^6 samples.

The input for each register comes from its associated gating card circuit. The 38 BCD output lines are routed to a common data bus by a signal on READOUT bus (a logical "0" on the READOUT bus selects a register) which selects the appropriate register. The common data bus is discussed in more detail in Section A.6.

The reference register is similar to the other 15 except that the "8" bit outputs from the highest 5 counters are routed to the sampling card to operate the AUTO-SHUTOFF circuitry for 10^5, 10^6, 10^7, 10^8 and 10^9 counts.

A.5 SAMPLING, TIME AND CONTROL

The sampling card contains circuitry for: 1) sampling, 2) timing, and 3) controlling the acquisition of the distributions. Figure A11 is a schematic of the sample timing circuit. This consists of a 2 MHz crystal oscillator and a frequency dividing chain to obtain the various sampling frequencies which are selected by a 10 position selector switch located on the front panel. The sampling waveform is a square wave which may be varied from 2 KHz to 2 MHz in a 1, 2, 5 sequence and is routed to the gating card.

Figure A12 is a schematic of the timing and control circuitry. The timing circuit produces an AUTO-SHUTOFF signal to reset the count enable which inhibits the gating of counts to the accumulator. The AUTO-SHUTOFF stops the data collection when the reference counter reaches the desired power of 10 as selected by a switch on the front panel. This switch also sets the decimal point on the display so that in the APD mode the percentage of time that each level is exceeded is displayed directly.

Before each distribution is taken, the control switch is switched to RESET. This sets each register in the accumulator to 9,999,999,999 and resets the two J-K flip-flops on this card (i.e., the Q output set to "0"). It also resets circuits on the printer Control Card (see Section A.6). When the control switch is switched to COUNT and the first count reaches each register, the register switches to 0 and the "8" bits of all the counters switch from "1" to "0". This transition clocks a "1" to the output of the first J-K flip-flop.

Some time later, the "8" output from the selected decade changes to a "1" and then, when the most significant 9 changes to a 0 (e.g., if 10^5 counts

are selected, when the count goes from 99,999 to 100,000) the "8" bit changes from "1" to "0". This transition toggles the first flip-flop (1 to 0) and causes the Q output of the second flip-flop to change from a "0" to a "1" which resets the COUNT ENABLE signal and stops the data collection process. In the manual mode, the two flip-flops are continuously cleared and the count is controlled by the COUNT-OFF-RESET switch. There are also components on the card for a DATA system to control the count but to date, these have not been used.

We presently operate the system with the control switch. We first switch to RESET and then to COUNT and use the AUTO-SHUTOFF to stop the data collection. The system then automatically outputs the contents of each register in the accumulator to the display and on the printer.

A.6 DISPLAY AND OUTPUT CONTROL

This Section consists of the circuits that route the data from the accumulator to the LED display and to the printer. The circuits on the METER-AUDIO card that is used to monitor the input signal are also included.

Figure A13 is a schematic of the data control circuitry. The 2 KHz signal from the sampling card is divided down to 2 Hz by a frequency divider chain to operate the printer. When the RNA is switched to RESET, the J-K flip-flop and the binary counter are cleared. This selects the reference register to be displayed through the one-of-16 decoder. As well, the AUTO-SHUTOFF goes to a "1". In normal operation after a distribution has been measured, the AUTO-SHUTOFF goes to "0" and clocks a "1" through the J-K flip-flop. This enables the 2 Hz pulses to start the binary counter. The output of the binary counter selects the first register of the accumulator by putting a "0" on one output of the one-of-16 decoder which lights the associated LED. It also provides the address of this register to the printer through the binary/BCD decoder. After the register has been selected and its output placed on the output data bus, a pulse from the one-shot acts as a print command and prints the data along with the register number. This sequence is repeated until the data from all 16 registers have been printed. When the binary counter cycles to 0 (most significant bit), the J-K flip-flop toggles to 0 and stops the 2 Hz pulses from getting through the NAND gate to advance the binary counter.

If the MANUAL READ switch is "ON", a signal inhibits the output from the one-of-16 decoder and the registers are selected by switches on the front panel. This mode is usually only used for test purposes.

Figure A14 is a schematic of data flow from the accumulator to the display and printer for one of the 38 bits and for three of the 16 registers. The circuitry for all bits and registers is identical. For each of the 38 data outputs, there is a common data bus linking the 16 registers. The data from a particular register is put on the data bus whenever that register is selected by a signal (0 volts) on the readout bus for that register. The readout bus is common to all the outputs of a particular register whereas the common data bus is common for one bit of all registers. The common data bus is a high impedance output operating at TTL logic levels ("1" ≡ 5V and "0" ≡ 0V). The output goes through two stages of level conversion. The

first stage converts the TTL levels to ("1" ≡ -12 V and "0" ≡ 0V). This output may be used for some peripheral devices (printers, tape recorders). The second stage of level conversion converts back to TTL levels to drive the LED display and the Fluke printer.

The LED display which displays the data on the data bus consists of ten sets of decoder drivers and 7 segment LED numeric displays. There are also inputs from the AUTO-SHUTOFF circuitry of the sampling card to set the decimal point and suppress display of zeroes to the left of the decimal point. The decimal point is used in the APD mode to display the percentage of time that each input level is exceeded. A front panel pushbutton switch (DISPLAY TEST) is included to test the display. When the switch is pressed, every segment of each display is lit, thus a simple inspection of the unlit segments detect LED or decoder/driver malfunctions.

Figure A15 is a schematic of the METER/AUDIO card. This card monitors the input signal at the output of the detector and is not in the data path and does not affect the measurements. A particular detector output is selected by a make-before-break switch (DETECTOR) and fed through a buffer amplifier. The output of the buffer goes to 1) an audio amplifier, and 2) a log amplifier. The audio amplifier is used to drive a set of earphones for aural monitoring of the input signal. The log amplifier produces a meter reading from +4 dB to -16 dB where 0 dB represents 0.5 volts output from the detector. The highest tripping point from each stage is 0.5V and the others are 0.25V at (-6 dB) and 0.125V at (-12 dB). This meter may be used as an indicator for the adjustment of the input level to the RNA before a distribution is acquired. For example, if Level one is being exceeded, then we may be clipping the higher levels of the input signal and the input should be reduced, and if the highest level being exceeded is Level 13, then the input level should be increased for a more accurate measurement.

A.7 POWER SUPPLY

The power supply for the RNA consists of 3 power supply modules as shown in the schematic of Figure A16. Two of the modules are Datel Model UPM 5/2000 power supplies, one is for the display which draws 1.3 amps and the other is for the rest of the 5 volt logic which draws 1.4 amps. The third unit is an acdc Electronics Inc. Model 12 D0.4 power supply which is used to power the $\pm$12 volts for the detector circuitry and the level converters. The "power-on" switch and 4 LED's which monitor the power bus voltages are located on the front panel. Overall the RNA consumes about 15.5 watts of power.

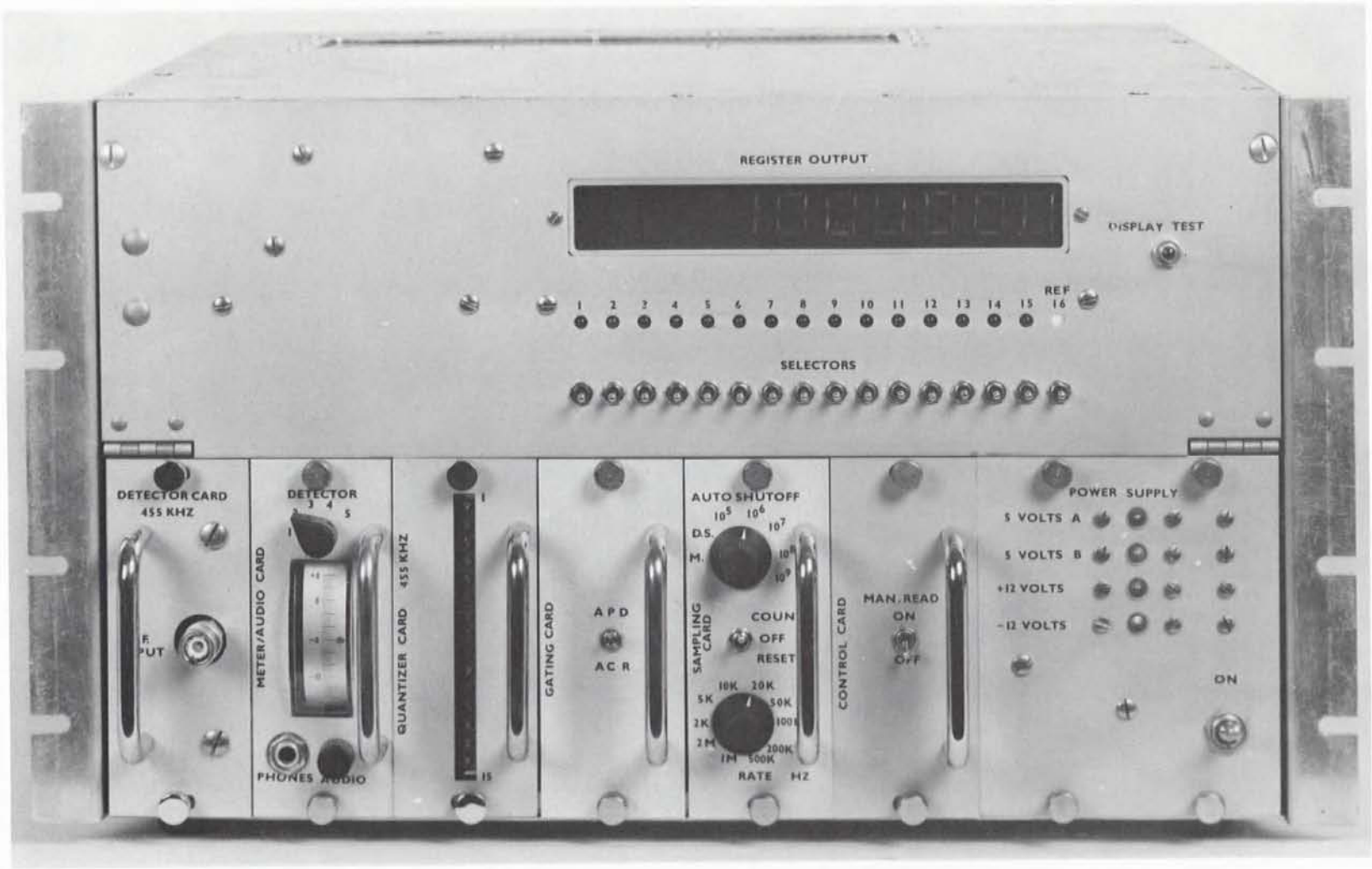

Figure A1. Photograph of the Front Panel

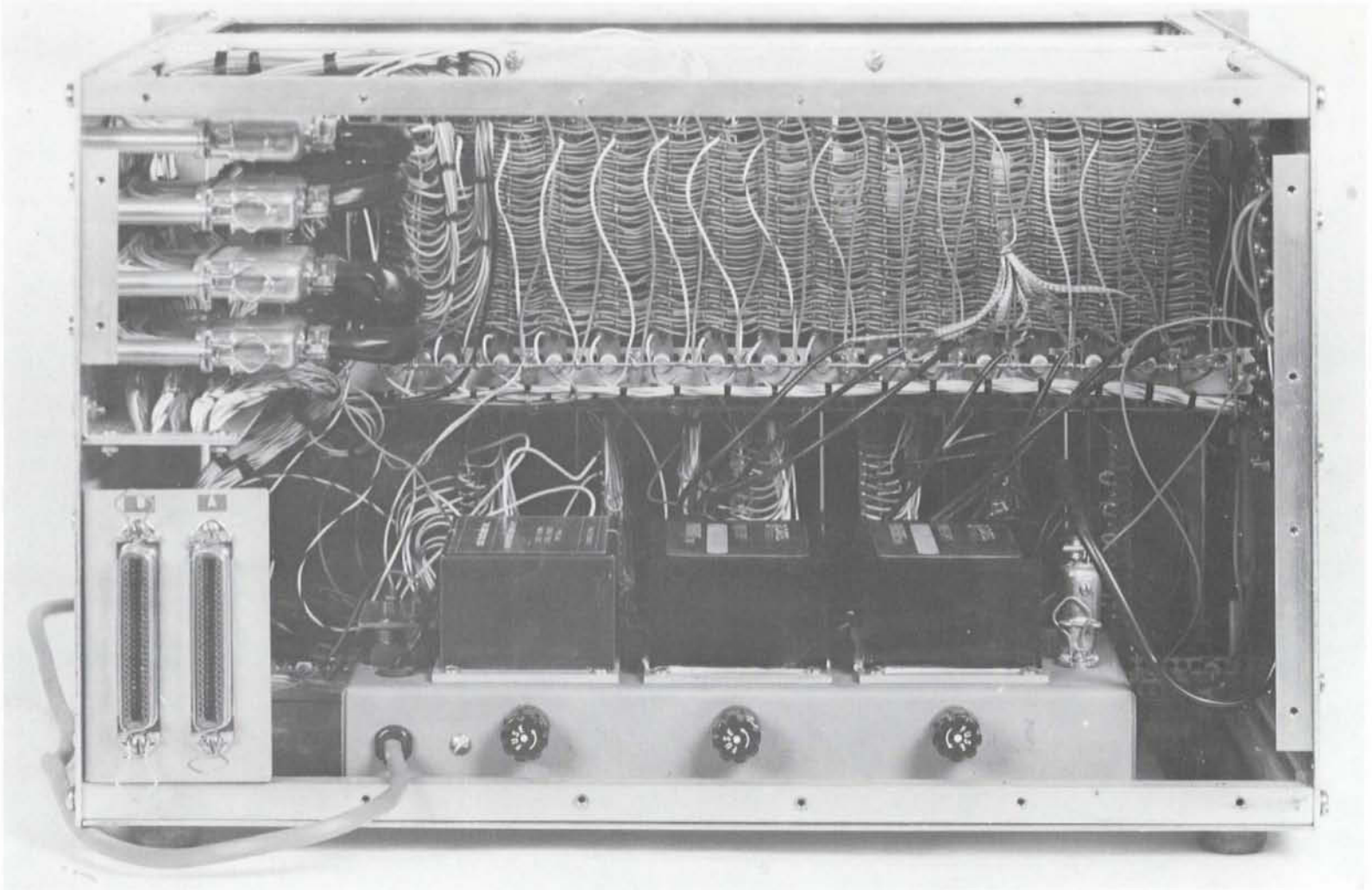

Figure A2. Photograph Showing the Physical Layout

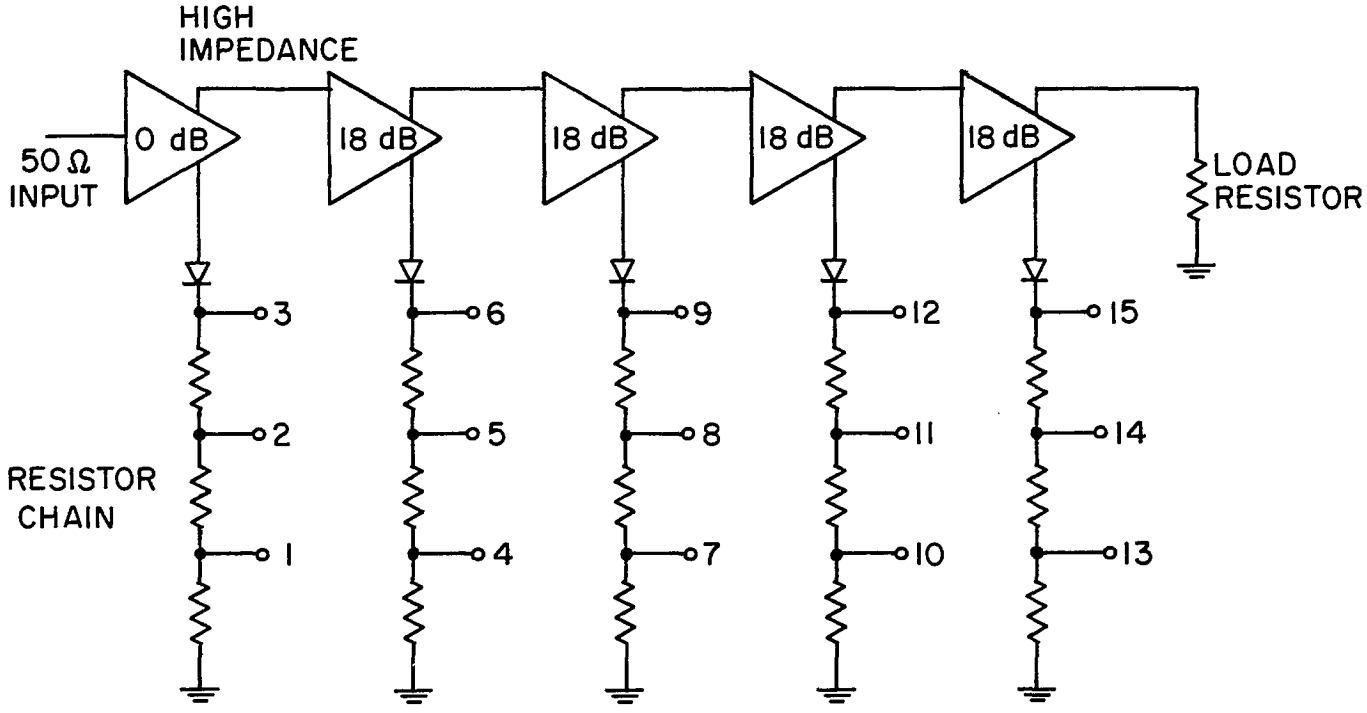

Figure A3. Overall Schematic of the Detector Circuitry

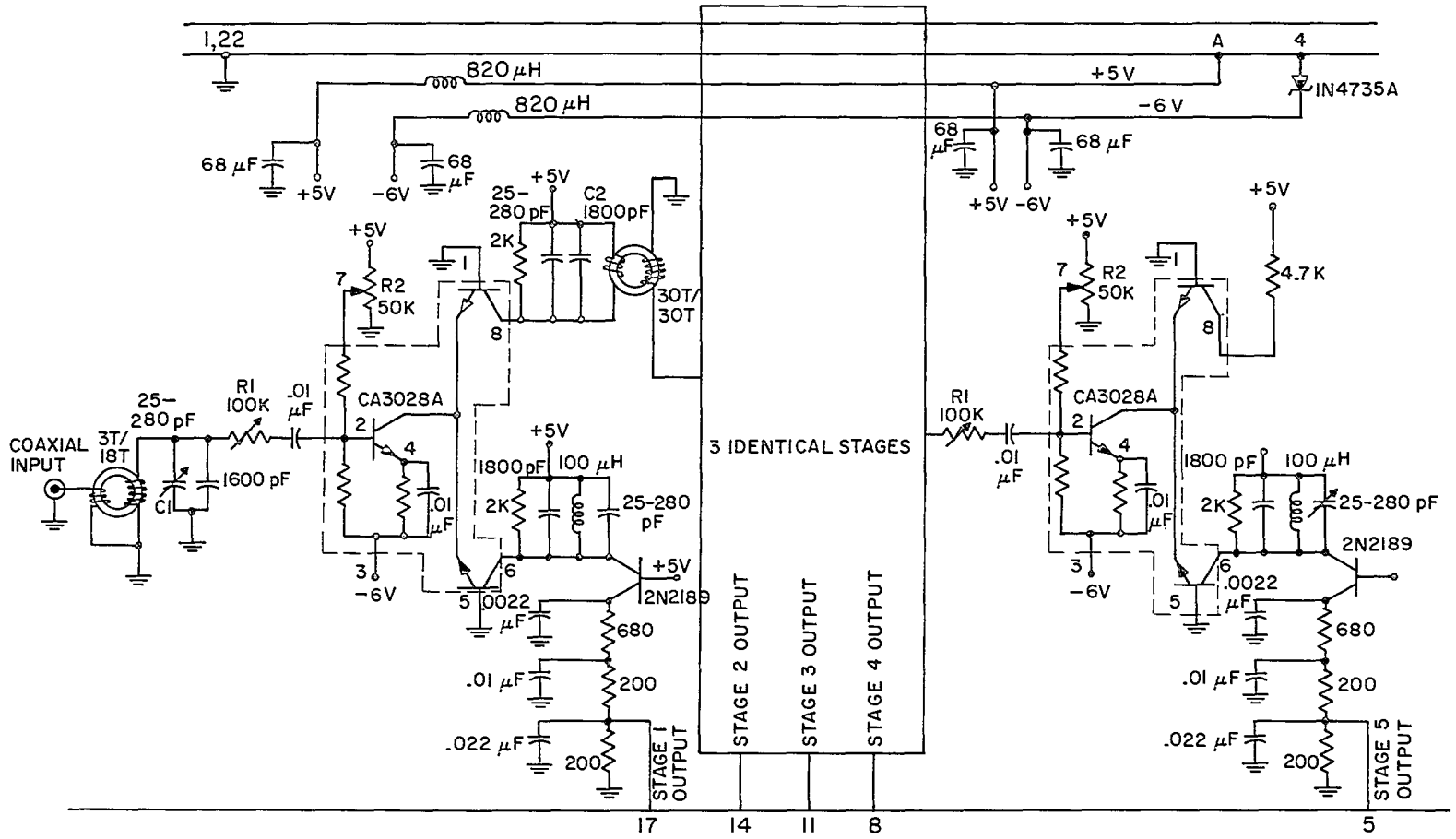

Figure A4. Schematic of the 455 KHz Detector

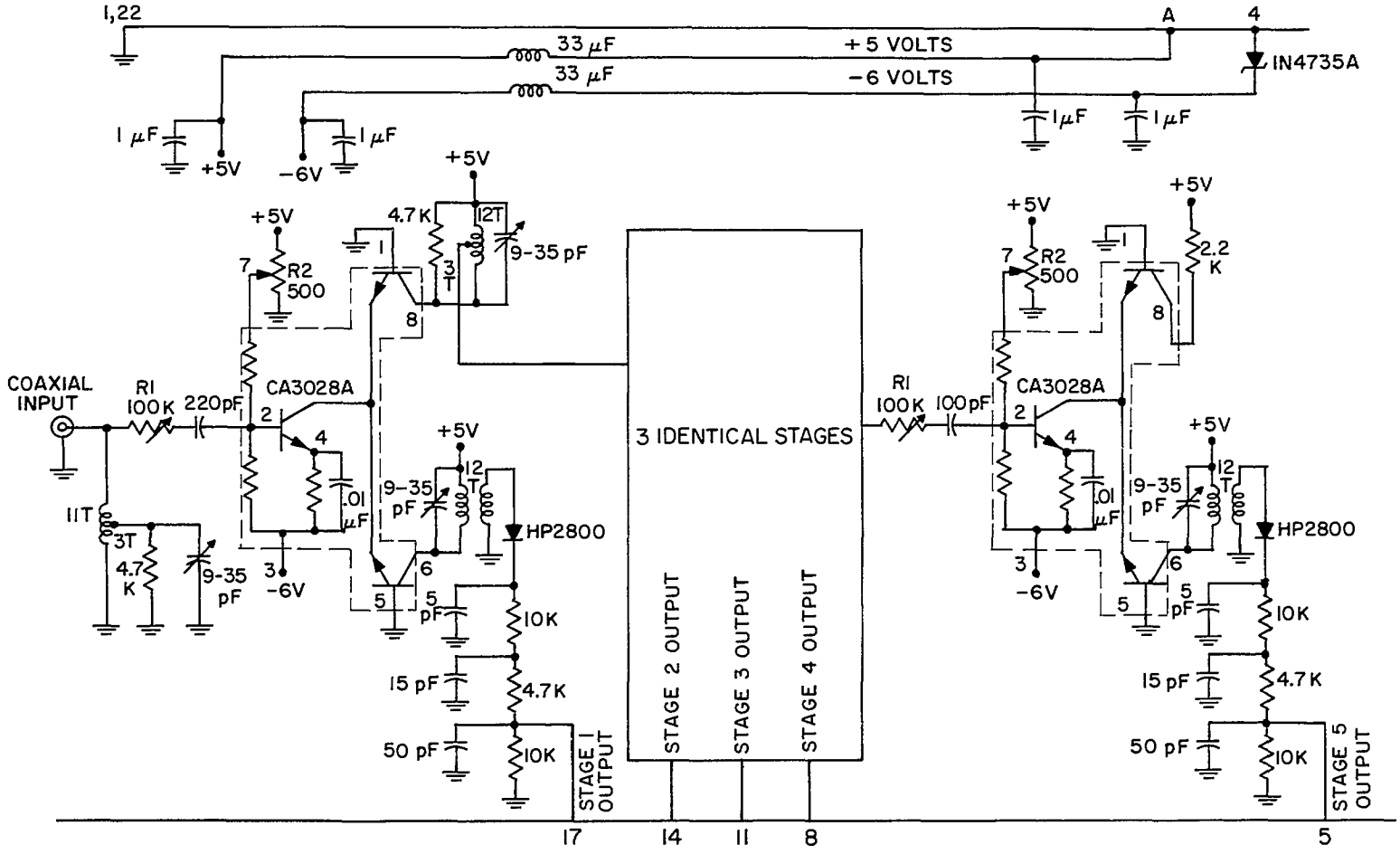

TOROIDS INDIANA GENERAL CF101 Q2 MATERIAL

Figure A5. Schematic of the 20.5 MHz Detector

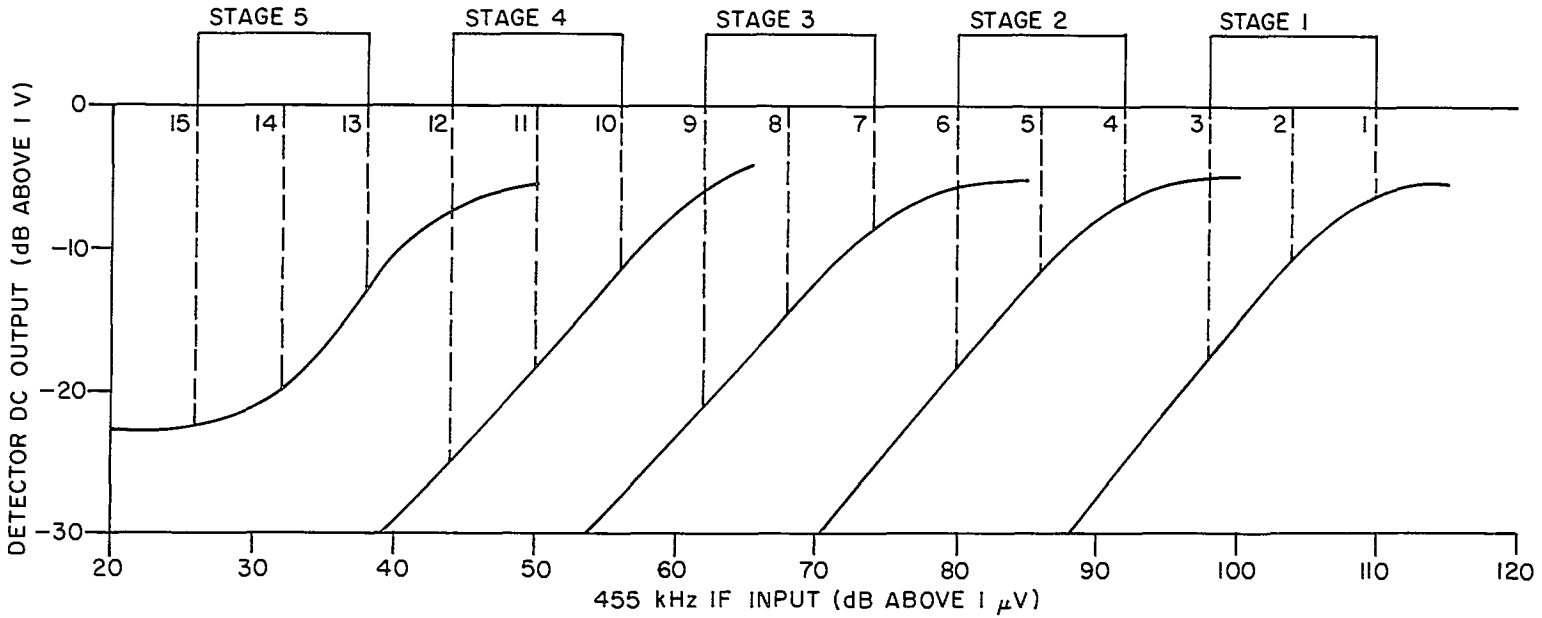

Figure A6. I/O Characteristics of the 455 KHz Detector

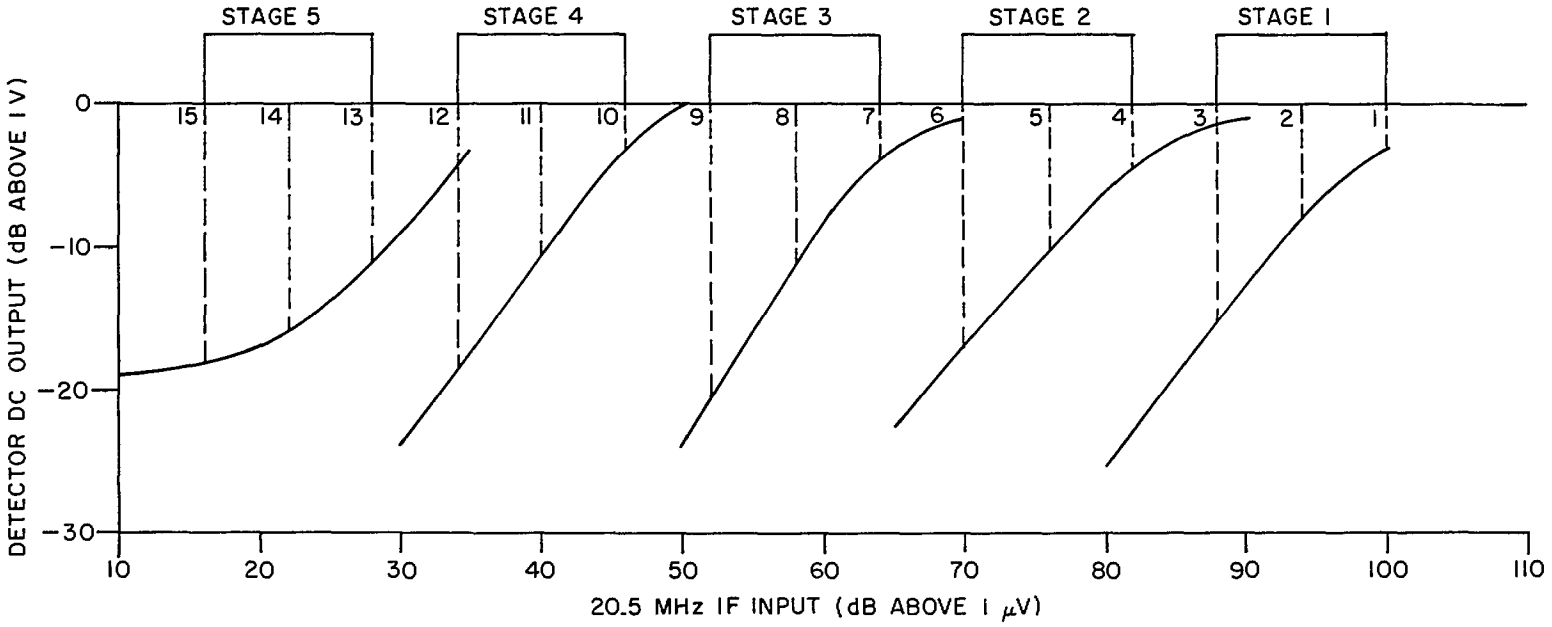

Figure A7. I/O Characteristics of the 20.5 MHz Detector

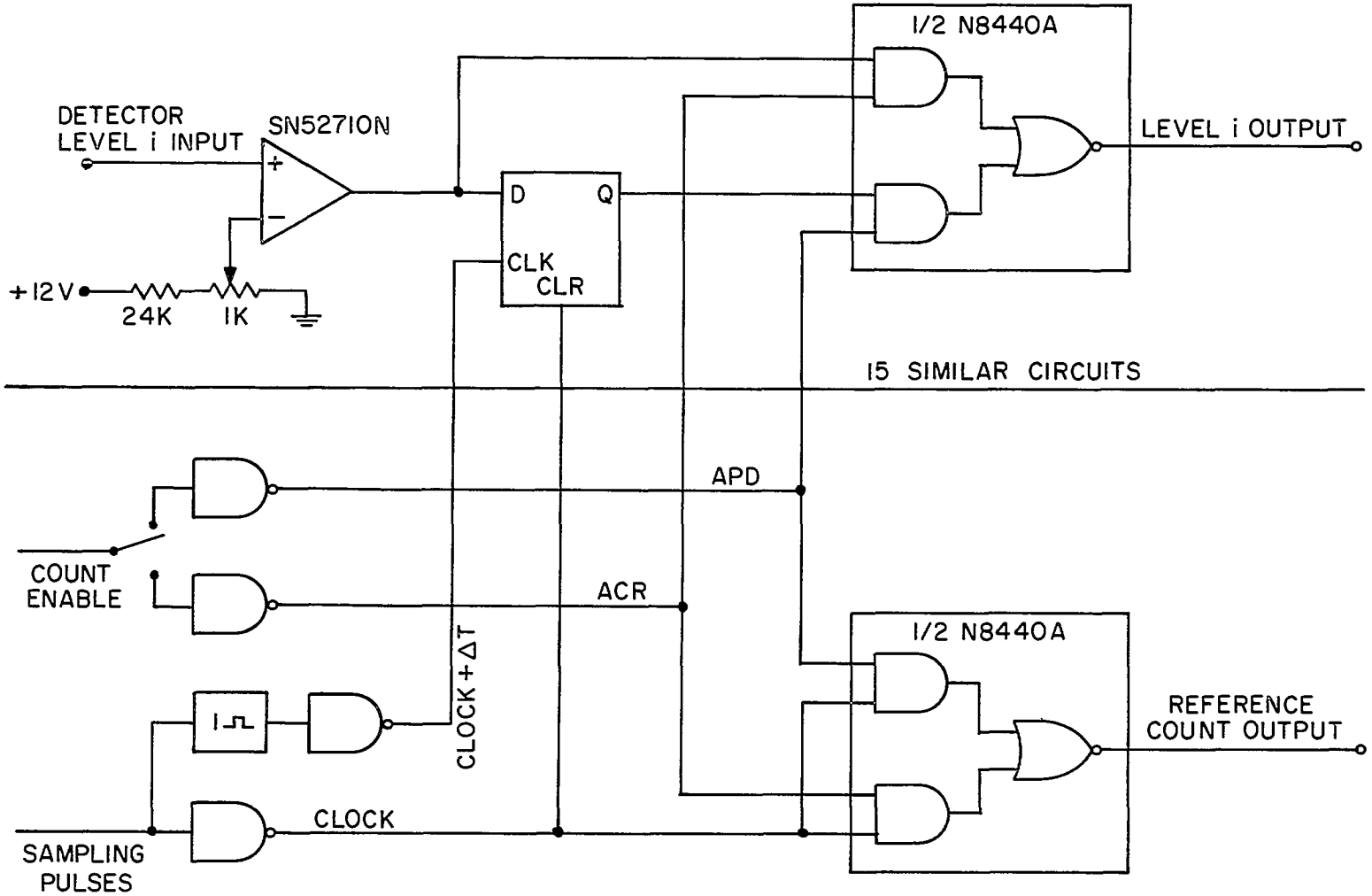

Figure A8. Block Diagram of the Digitizer

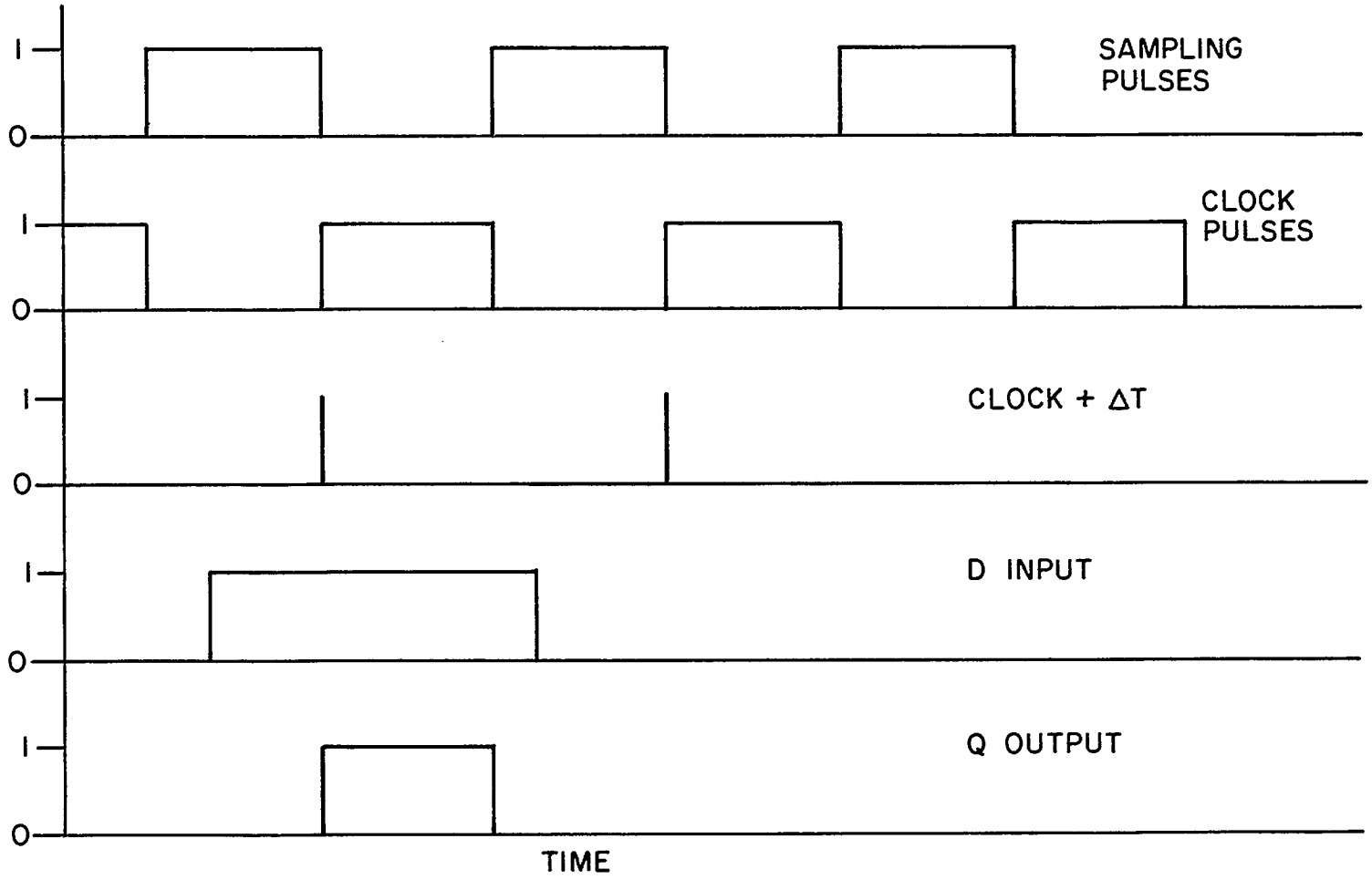

Figure A9. Timing Diagram

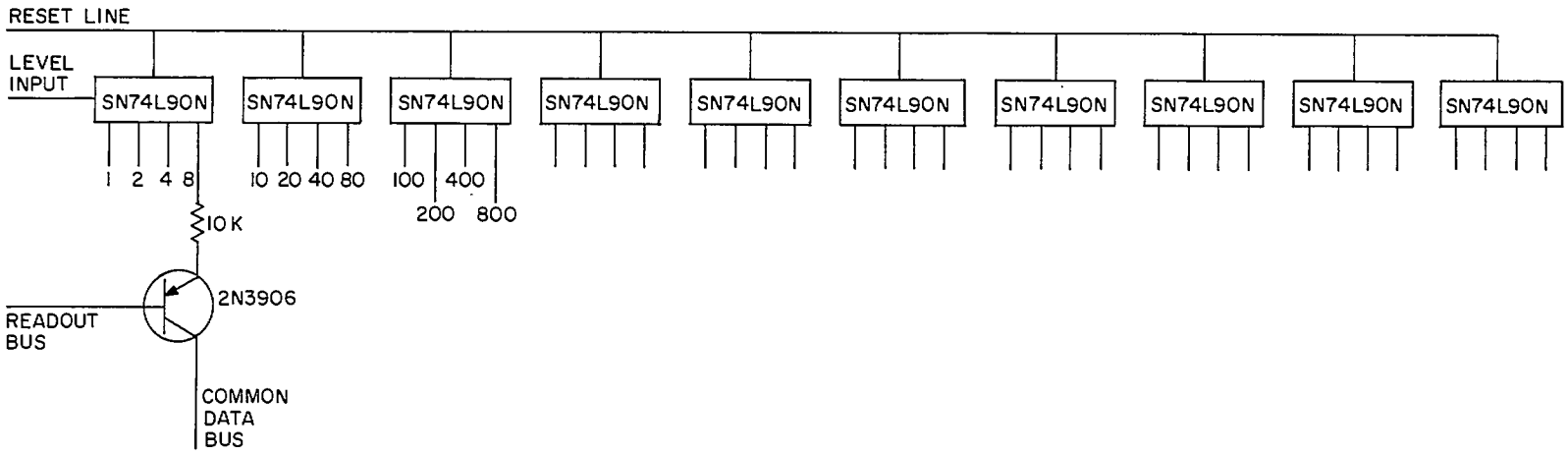

Figure A10. Schematic of a Register Card

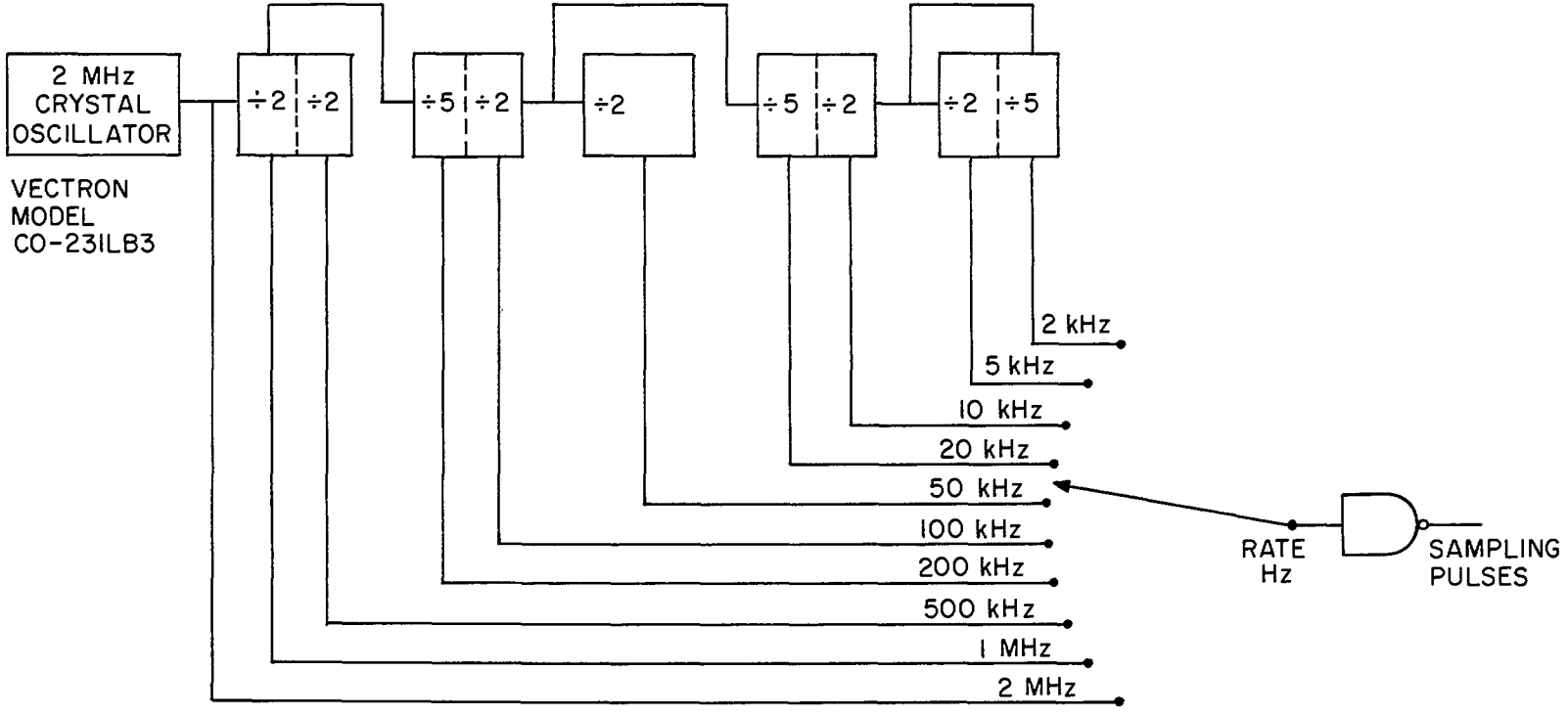

Figure A11. Schematic of the Sampling Circuitry

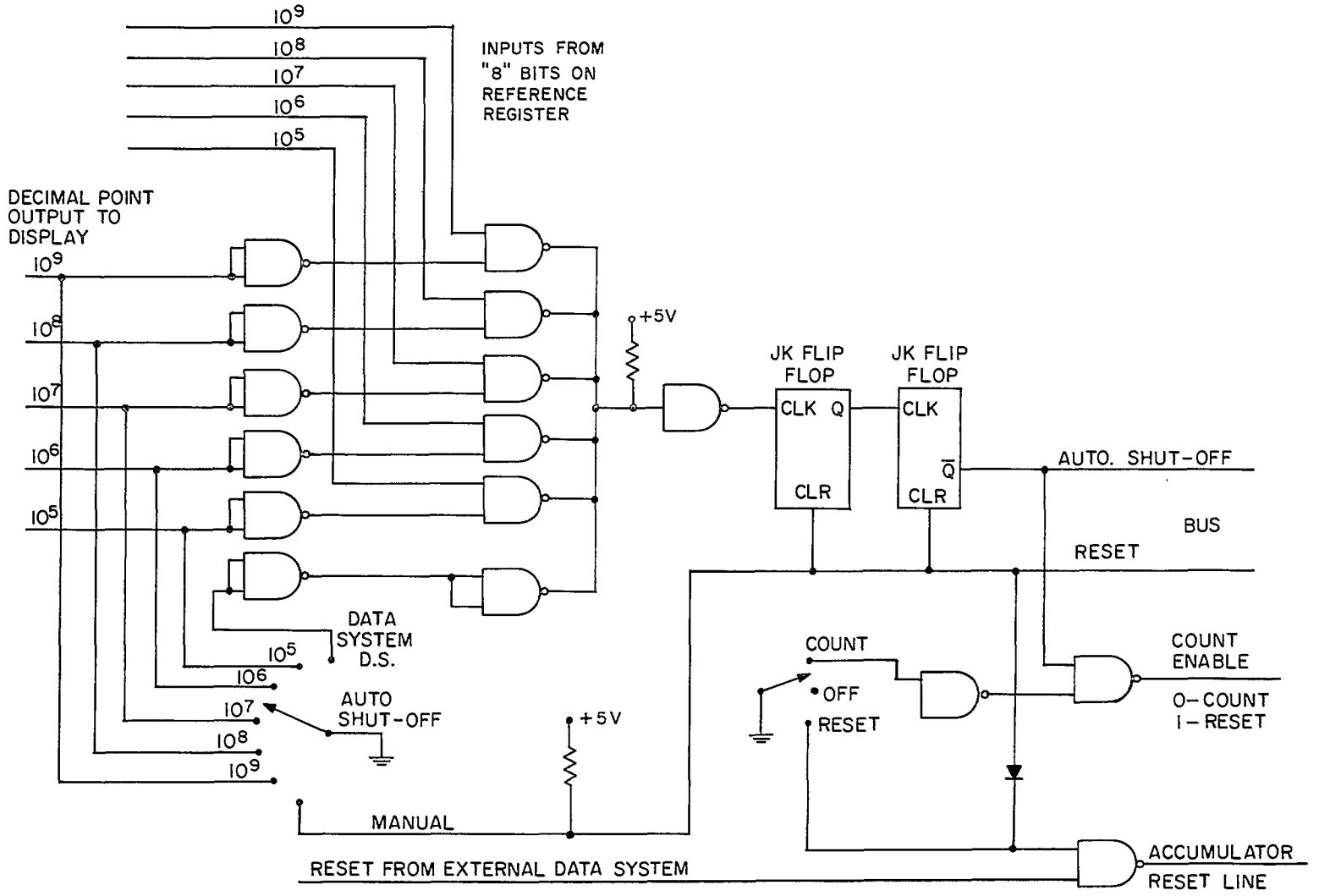

Figure A12. Schematic of the Timing and Control Circuitry

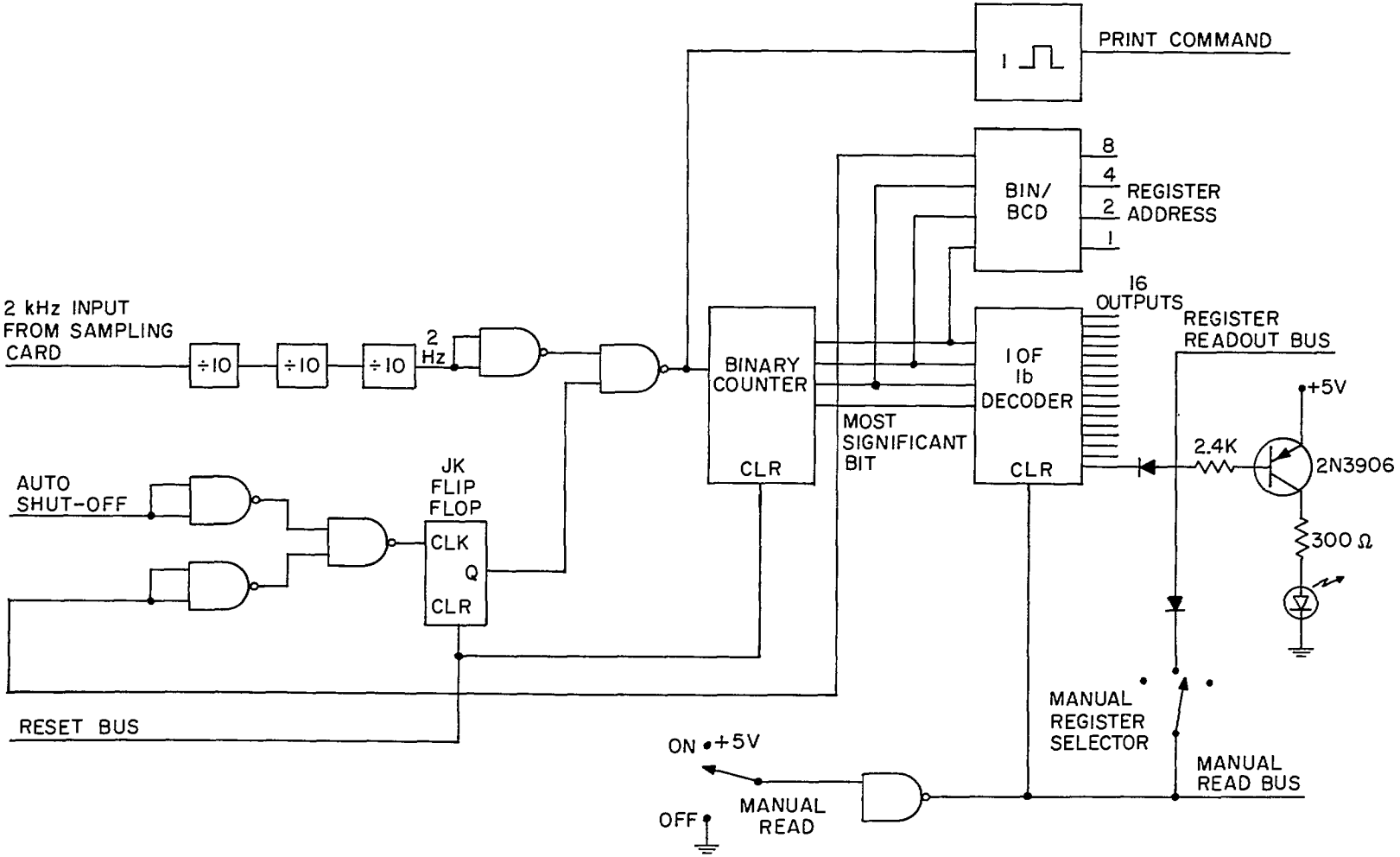

Figure A13. Schematic of the Output Data Control Circuitry

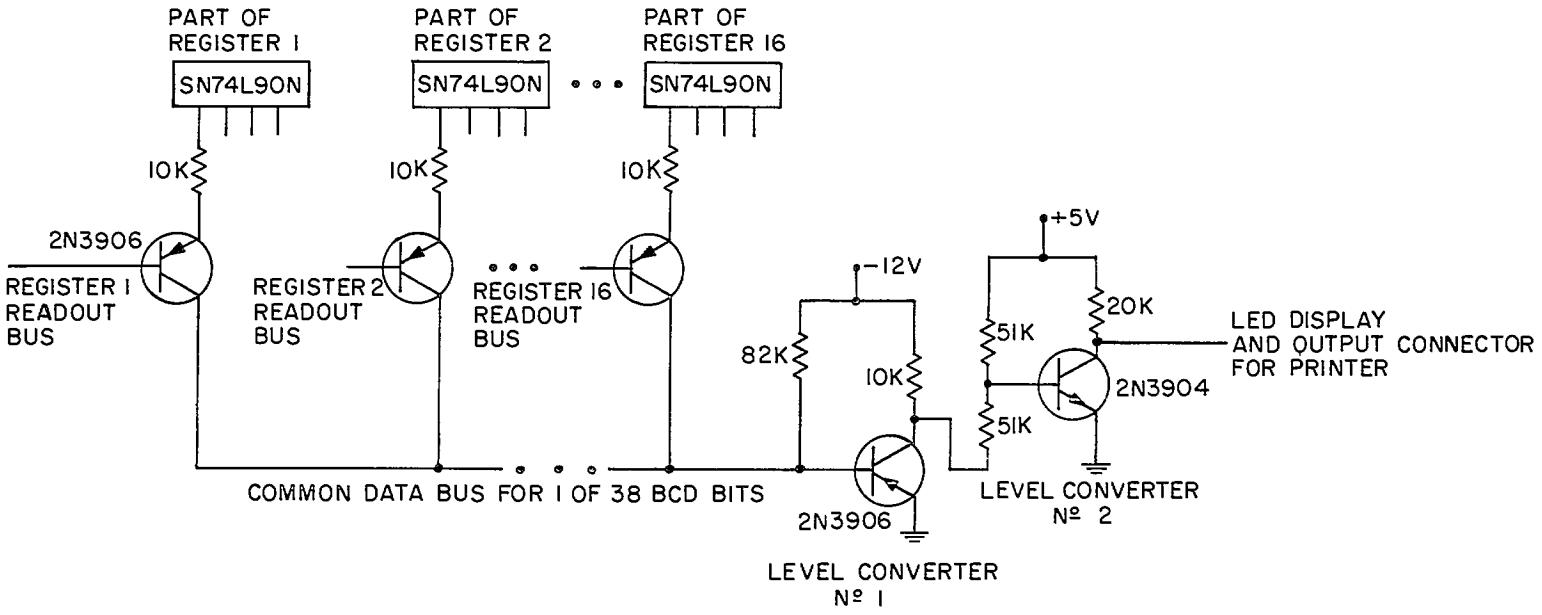

Figure A14. Schematic of the Data Flow from Accumulator to Display and Printer

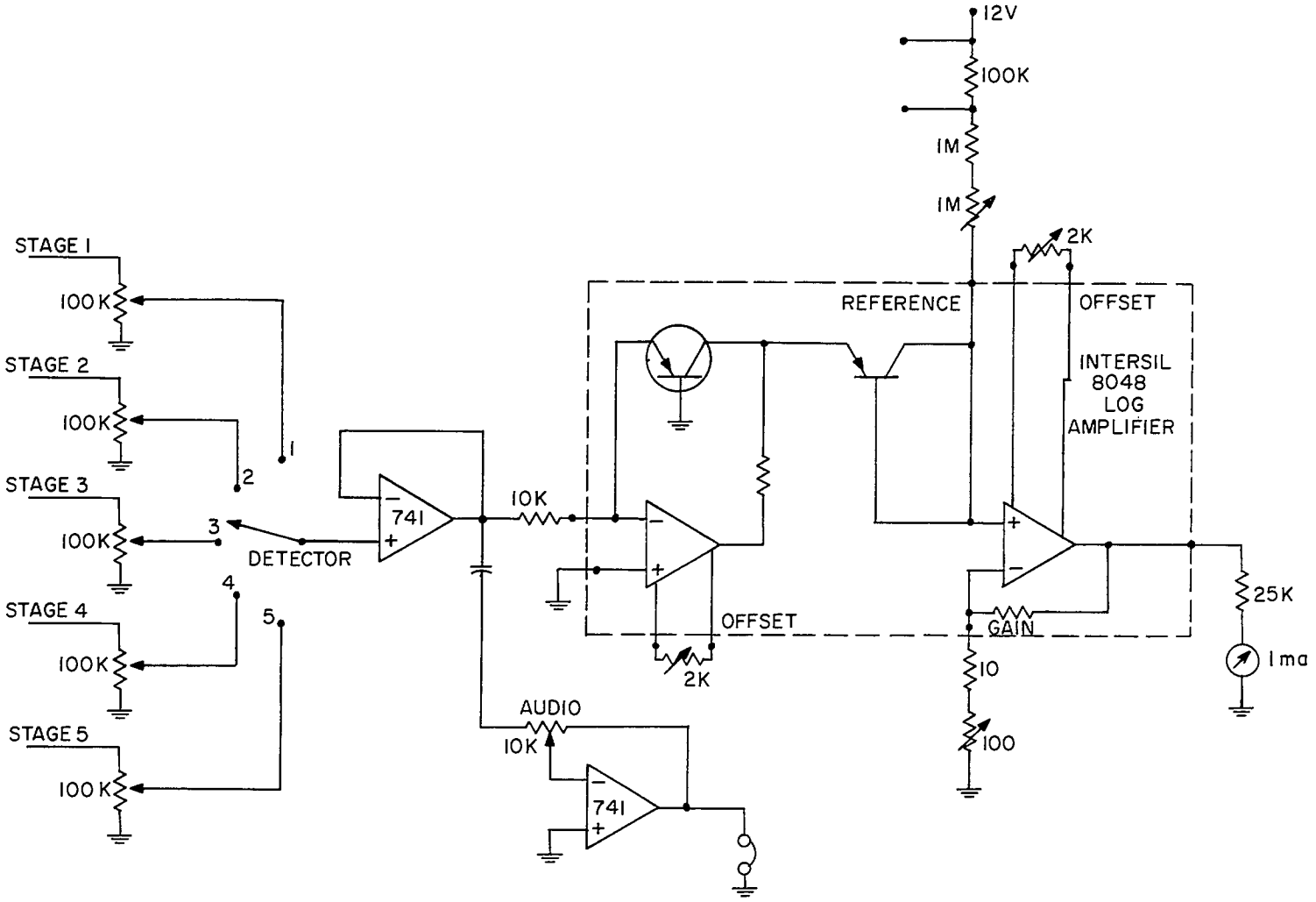

Figure A15. Schematic of the Meter/Audio Card

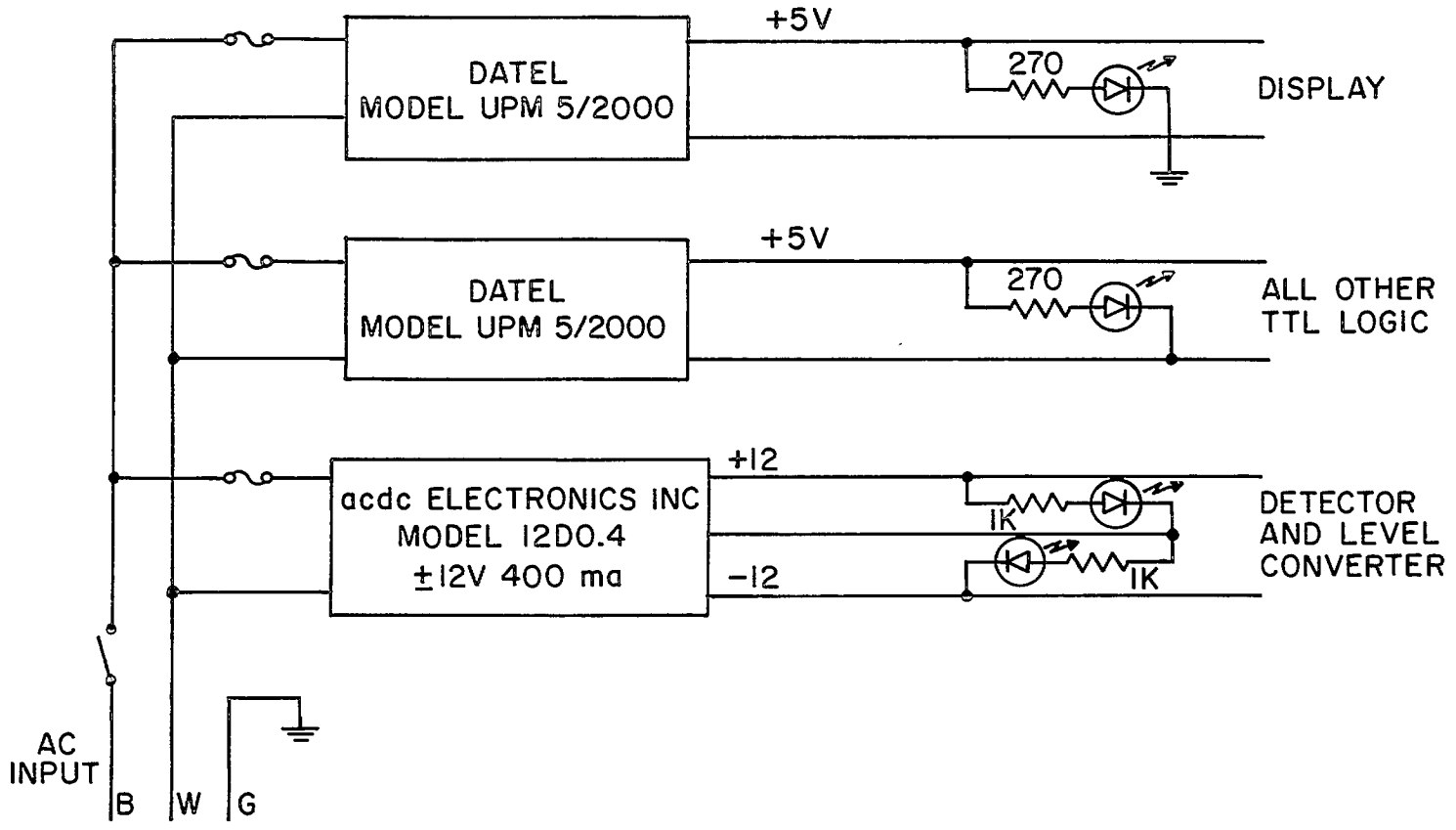

Figure A16. Schematic of the Power Supply

A P P E N D I X B

Operating Procedures

INTRODUCTION

This Appendix describes the typical operating procedures for this equipment when it is used with either the Singer NM-26T or NM 37/57 receivers, and the Fluke printer i.e. the complement of equipment now available. In this Appendix we will assume a general knowledge of the operation of the two receivers, and that the receiver and noise analyzer have been calibrated as a system.

OPERATION WITH THE SINGER NM-26T RECEIVER

Figure B1 shows a system configuration with the Singer NM-26T receiver, the Radio Noise Analyzer, the Fluke printer, and an optional oscilloscope for a time display of the noise. The following steps detail the operation of this equipment.

1. a) Connect the antenna to the receiver RF input.
   b) Connect the IF output of the receiver to the RNA input of the 455 kHz detector card.
   c) Connect the Fluke printer to the RNA output.
   d) Connect the oscilloscope to scope output of receiver (optional).

2. Set up Receiver

   a) Tune receiver to the desired signal free frequency.
   b) Calibrate receiver.
   c) Tune function switch to "Noise".
   d) Set the attenuator for an on-scale reading on the RMS meter, i.e. above set noise.
   e) Turn function switch to "Peak" and set "Peak" adjustment to give ≈ 15 dB reading. (This gives a fixed gain receiver, i.e. no AGC).

3. Set up RNA

   a) Set MAN READ Switch to OFF.
   b) Set COUNT-OFF-RESET switch to RESET.
   c) Decide whether you want an APD or an ACR and set switch on gating card.
   d) If APD, set AUTO SHUT to desired number of samples say 10^6 and set RATE switch to say 20 kHz sampling rate.
   e) If ACR, set any combination of AUTO SHUT OFF and RATE switches to give desired time window say 100 seconds.
   NOTE: In the ACR mode the sampling rate has no effect on the ACR.

f) Set all the SELECTOR switches to the mid-position.

4. To measure the desired distribution set the COUNT-OFF-RESET switch to COUNT. The selector display automatically monitors the reference register until the required number of samples has been taken. The contents of the registers are then automatically dumped onto the printer in sequence and the equipment stops. To measure another distribution simply set the COUNT-OFF-RESET switch to RESET and after deciding on type of distribution and frequency etc. set it to COUNT for next distribution.

OPERATION WITH THE SINGER NM 37/57 RECEIVER

Figure B2 shows a system configuration with the Singer NM 37/57 receiver, the Radio Noise Analyzer, the Fluke printer, and an optional oscilloscope for a time display of the noise. The following steps detail the operation of this equipment.

1. a) Connect the antenna to the receiver RF input.
   b) Connect the IF output of the receiver to the RNA input of the 20.5 MHz detector card.
   c) Connect the Fluke printer to the RNA output.
   d) Connect the oscilloscope to the Y OUTPUT of the receiver (optional).

2. Set up the Receiver

   a) Tune the receiver to the desired signal free frequency.
   b) Calibrate the receiver.
   c) Turn the FUNCTION switch to "FI", AFC to "OFF", and AUDIO to "AM".
   d) Set the BANDWIDTH switch for the desired bandwidth.
   e) Set the attenuator for an on scale reading on the meter, i.e. above set noise.

3. The set up and operation of the RNA is identical to that described in the previous Section. Since the IF output is independent of the AGC circuit of the receiver, the receiver function switch may be in any position other than CAL or BFO.

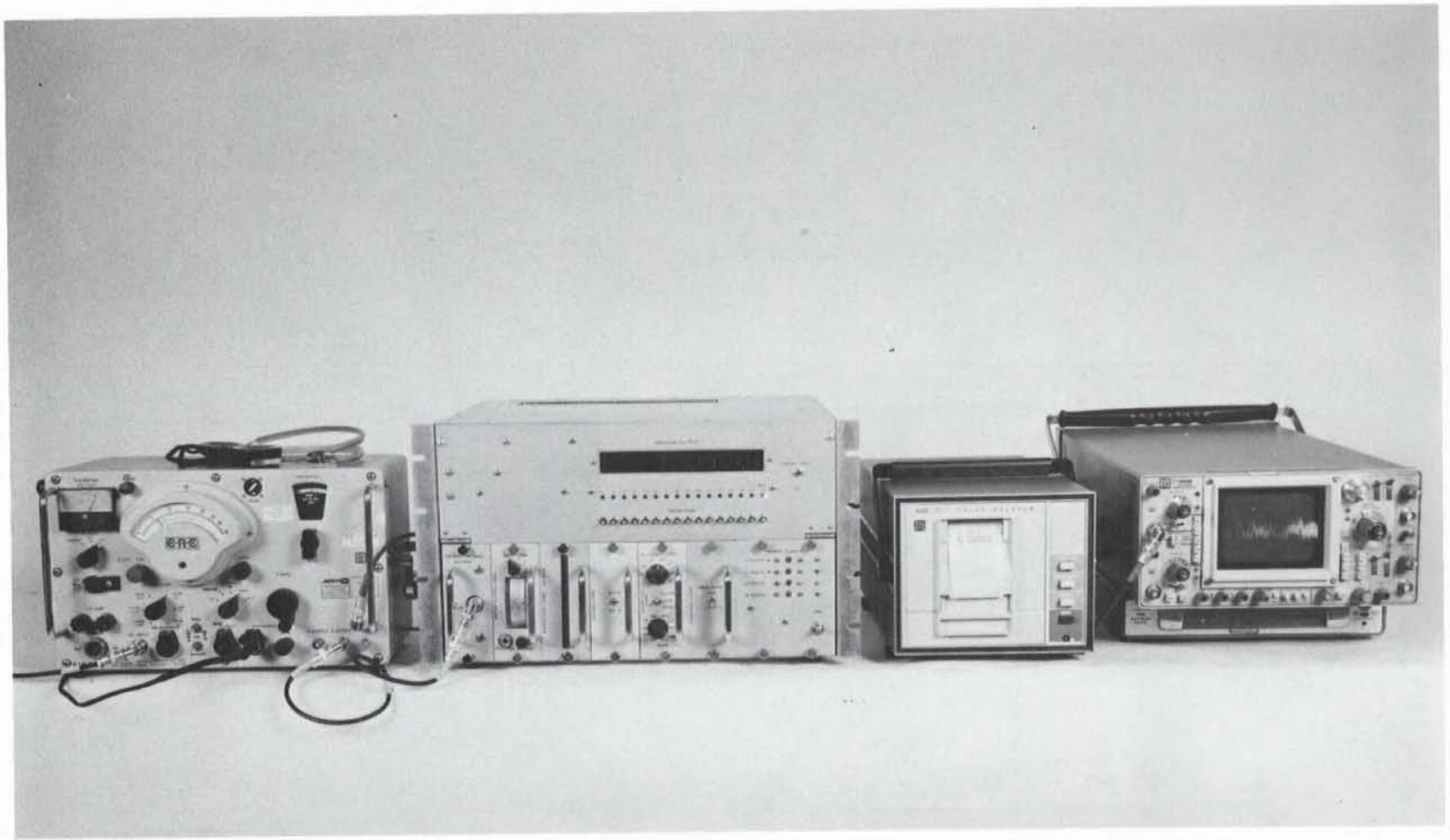

Figure B1. System Configuration with Single NM-26T Receiver

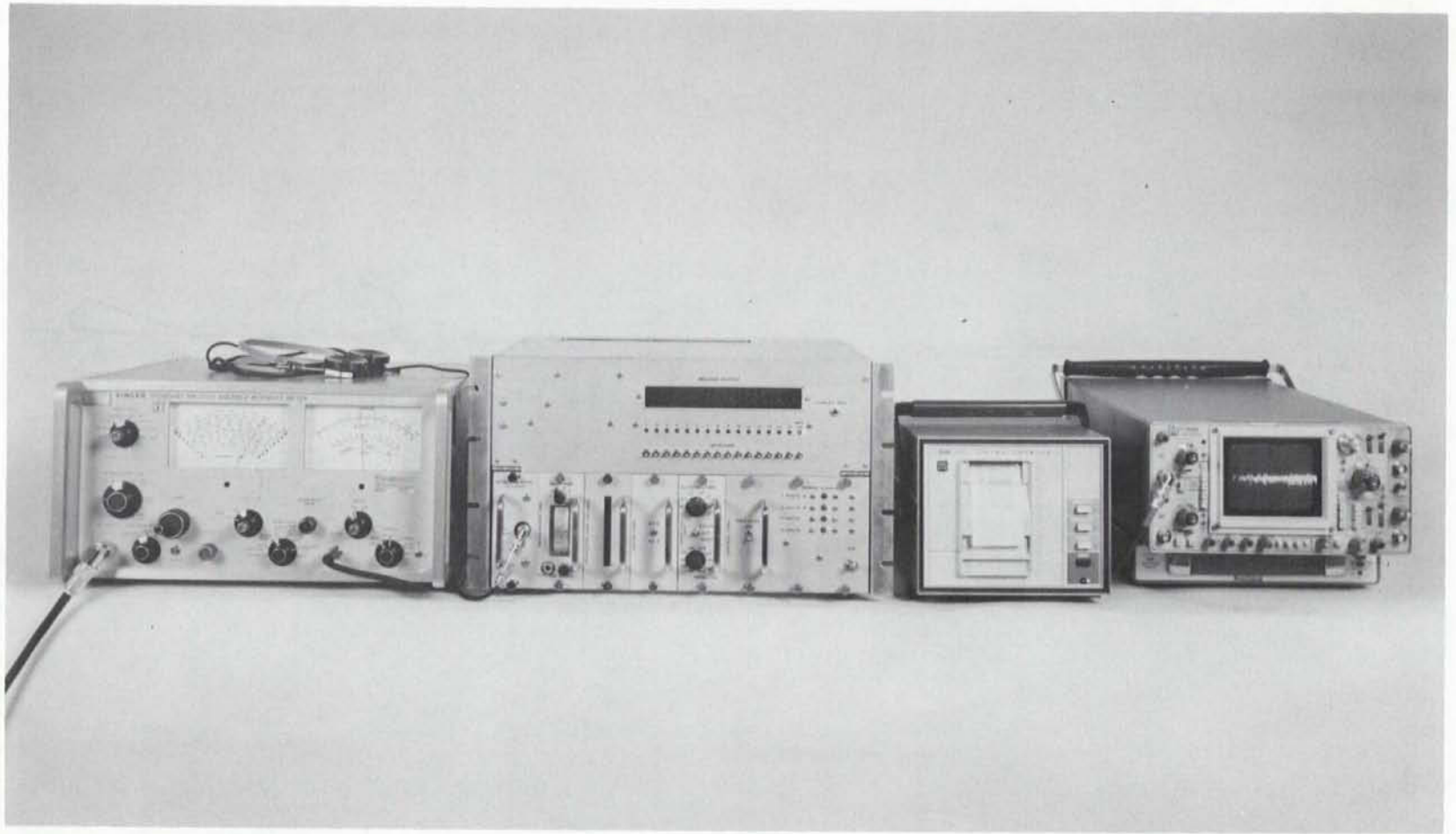

Figure B2. System Configuration with Singer NM 37/57 Receiver

CRC DOCUMENT CONTROL DATA

1. **ORIGINATOR:** Department of Communications/Communications Research Centre

2. **DOCUMENT NO:** CRC Technical Note No. 696

3. **DOCUMENT DATE:** January 1979

4. **DOCUMENT TITLE:** A Radio Noise Analyzer

5. **AUTHOR(s):** W.R. Lauber and J.M. Bertrand

6. **KEYWORDS:** (1) Radio
(2) Noise
(3) Statistical

7. **SUBJECT CATEGORY (FIELD & GROUP: COSATI)**

17 Navigation, Communications, Detection, and Countermeasures

17 02 Communications

8. **ABSTRACT:** This report describes equipment which has been constructed at the Communications Research Centre (CRC) to measure statistical distributions of radio noise. The Analyzer in its present configuration may be used with either of two receivers, thus giving a frequency coverage from 150 kHz to 1 GHz. The equipment can make measurements of Amplitude Probability Distribution's (APD's) and Average Crossing Rate (ACR) characteristics; however, plans are given for modifying the equipment to enable measurements of Pulse Spacing and Pulse Duration Distributions. The results of system-performance tests for both gaussian and impulse noise are given. Appendices are included which describe the detailed circuitry and the operational procedures of the Analyzer.

9. **CITATION:**

LAUBER, W. R.
--A radio noise analyzer.

LKC
TK5102.5 .R48e #696
c.2
A radio noise analyzer

DATE DUE
DATE DE RETOUR

LOWE-MARTIN No. 1137

CRC LIBRARY/BIBLIOTHEQUE CRC
TK5102.5 R48e #696 c. b
Lauber, W. R.

INDUSTRY CANADA / INDUSTRIE CANADA
212163

Government of Canada
Gouvernement du Canada